Journal of Food and Drug Analysis

Volume 31 | Issue 2 Article 5

The inhibitory effect of quercetin-3-glucuronide on pulmonary injury in vitro and in vivo

ORIGINAL ARTICLE

The inhibitory effect of quercetin-3-glucuronide on pulmonary injury *in vitro* and *in vivo*

Pei-Rong Yu [a], Jen-Ying Hsu [a,b], Chiao-Yun Tseng [a], Jing-Hsien Chen [a,c,1], Hui-Hsuan Lin [c,d,*,1]

[a] Department of Nutrition, Chung Shan Medical University, Taichung City, 40201, Taiwan
[b] Department of Biochemistry and Molecular Vascular Biology, Kanazawa University Graduate School of Medical Sciences, Kanazawa, Japan
[c] Clinical Laboratory, Chung Shan Medical University Hospital, Taichung City, 40201, Taiwan
[d] Department of Medical Laboratory and Biotechnology, Chung Shan Medical University, Taichung City, 40201, Taiwan

Abstract

Pulmonary injury is defined as a progressive inflammation. Extensive pro-inflammatory cytokines are secreted from alveolus, associated with the production of reactive oxygen species (ROS) and apoptosis. The model of endotoxin lipopolysaccharide (LPS)-stimulated lung cells has been applied to mimic the pulmonary injury. Some antioxidants and anti-inflammatory compounds can be used as chemopreventive agents of pulmonary injury. Quercetin-3-glucuronide (Q3G) has been showed to exert antioxidant, anti-inflammatory, anti-cancer, anti-aging and anti-hypertension effects. The aim of the study is to examine the inhibitory potential of Q3G on pulmonary injury and inflammation *in vitro* and *in vivo*. Firstly, human lung fibroblasts MRC-5 cells pre-treated with LPS were demonstrated to cause survival loss and ROS generation, were recovered by Q3G. Q3G also exhibited the anti-inflammatory effects on the LPS-treated cells with a reduction in the activation of NLRP3 [nucleotide-binding and oligomerization domain (NOD)-like receptor protein 3] inflammasome, leading to pyroptosis. Also, Q3G showed the anti-apoptotic effect in the cells might be mediated via inhibition of mitochondrial apoptosis pathway. To further explore *in vivo* pulmonary-protective effect of Q3G, C57BL/6 mice were intranasally exposed to a combination of LPS and elastase (LPS/E) to perform the pulmonary injury model. The results revealed that Q3G ameliorated pulmonary function parameters and lung edema in the LPS/E-induced mice. Q3G also suppressed the LPS/E-stimulated inflammation, pyroptosis and apoptosis in the lungs. Taken together, this study suggested the lung-protective potential of Q3G via downregulation of inflammation, pyroptotic and apoptotic cell death, contributing to its chemopreventive activity of pulmonary injury.

Keywords: Apoptosis, Inflammasome, Pulmonary injury, Pyroptosis, Quercetin-3-glucuronide (Q3G)

1. Introduction

Pulmonary injury may develop into acute respiratory distress syndrome (ARDS) or chronic obstructive pulmonary disease (COPD), which causes severe impairment of pulmonary function and respiratory failure in critically ill patients with high morbidity and mortality rates [1,2]. The classical characterization of pulmonary injury is hypoxemia, lung edema, neutrophil infiltration and release of pro-inflammatory cytokines [3]. Lipopolysaccharide (LPS), an endotoxin that is the major constituent of

Abbreviations: ROS, reactive oxygen species; LPS, lipopolysaccharide; Q3G, quercetin-3-glucuronide; NLRP3, nucleotide-binding and oligomerization domain (NOD)-like receptor protein 3; TLR4, toll-like receptor 4; NF-κB, nuclear factor kappa-light-chain-enhancer of activated B cells; IL, interleukin; TNF, tumor necrosis factor; ASC, apoptosis-associated speck-like protein containing a caspase recruitment domain; GSDMD, gasdermin D; Bcl-2, B-cell lymphoma 2; caspase, cysteine-aspartic proteases; Dex, dexamethasone; ELISA, enzyme-linked immunosorbent assay; SDS-PAGE, sodium dodecyl sulfate-polyacrylamide gel electrophoresis; H&E, hematoxylin and eosin; TUNEL, terminal deoxynucleotidyl transferase dUTP nick end labeling.

Received 7 September 2022; accepted 6 March 2023.
Available online 15 June 2023

* Corresponding author at: Department of Medical Laboratory and Biotechnology, Chung Shan Medical University, No. 110, Sec. 1, Jianguo N. Road, Taichung City, 40201, Taiwan. Fax: +(886) 4 23248171.
E-mail address: linhh@csmu.edu.tw (H.-H. Lin).
[1] These authors contributed equally to this study and therefore share corresponding authorship.

https://doi.org/10.38212/2224-6614.3453

the cell wall of gram-negative bacteria and also presented in tobacco smoke, is widely used to simulate clinically relevant pulmonary injury, in particular in ARDS [4,5]. It is well-known that LPS and its primary receptor, toll-like receptor 4 (TLR4), induces the myeloid differentiation primary response gene 88 (MyD88)-dependent pathway, and then leads to the activation of nuclear factor kappa-light-chain-enhancer of activated B cells (NF-κB) and/or mitogen-activated protein kinases (MAPKs) to modulate the release of pro-inflammatory cytokines, including interleukin (IL)-1β, IL-6 and tumor necrosis factor (TNF)-α [6].

In addition to inducing inflammatory mediators, LPS is reported to enhance the generation of reactive oxygen species (ROS), promoting oxidative stress [7]. Given previous studies have indicated the LPS-stimulated lung cells operate excessive production of ROS, then leading to activation of the nucleotide-binding and oligomerization domain (NOD)-like receptor protein 3 (NLRP3) inflammasome. The NLRP3 inflammasome is multi-protein complex composed of a NOD-like receptor, NLRP3 protein, apoptosis-associated speck-like protein containing a caspase recruitment domain (ASC) and pro-caspase-1, and can recognize a wide range of pathogens and damage-related molecules. The assembly of NLRP3 inflammasome regulates the activation of cysteine-aspartic proteases (caspase)-1, and sequentially triggers the release of pro-inflammatory cytokine IL-1β [8]. The activated caspase-1 cleaves not only pro-IL-1β but also pro-IL-18, finally leading to gasdermin D (GSDMD)-mediated pyroptotic cell death [9]. In the processes of pulmonary injury, LPS-induced oxidative stress highly correlates with the onset of apoptotic cell death, and thus antioxidants exhibit protection against LPS-evoked lung cell apoptosis, especially mitochondrial apoptotic pathway [10]. ROS have been explored to rise mitochondrial membrane permeability involving the molecular factors of B-cell lymphoma 2 (Bcl-2) protein family, causing the activation of caspase cascade [11]. Therefore, the evidences may provide a therapeutic strategy of ARDS and COPD to inhibit inflammation, oxidative stress and/or cell death in contribute to anti-pulmonary injury.

Quercetin-3-glucuronide (Q3G), which is the metabolite of quercetin, is one class of flavonoids found in fruits, vegetables and medicinal plants. Q3G is also the major quercetin conjugate in human plasma, in which quercetin is absent or undetectable, because it is rapidly conjugated with glucuronic acid after absorption from the small intestine [12,13]. Although studies have revealed that quercetin possesses anti-carcinogenic, anti-inflammatory, anti-thrombotic, anti-microbial, anti-viral and neuro-protective activities [14,15], it has poor bioavailability owing to its low water solubility, chemical instability and short biological half-life, reducing its efficacy in the food and pharmaceutical fields [16]. Better than the above-mentioned, most of the quercetin in foods and its metabolites are attached to a sugar molecule, and presence of sugar moieties can increase bioavailability due to the higher water solubility [17]. In recent studies, Q3G has attracted significant attention as an active compound with an active compound with biological functions containing antioxidant, anti-inflammatory, anti-cancer, anti-aging and anti-hypertension effects [18–23]. According to the potential benefits, Q3G is considered as a powerful phytochemical for disease prevention and health promotion.

Currently, there is no effective drug in prevention and treatment of pulmonary injury. Dexamethasone (Dex), an anti-inflammatory steroid, is commonly applied for clinical treatment of ARDS or other acute lung injury due to its favorable anti-inflammatory and immune-modulatory abilities. However, the use of the drug may lead to ARDS patients with severe hypersensitivity reactions, gastrointestinal toxicity and other side effects; thus, the efficacy of Dex isn't still satisfying [24]. Thus, it is imperative need to identify a promising agent with no adverse effect that beneficially improves lung function and prevents pulmonary injury. Moreover, a previous study has proven that Q3G exhibits anti-inflammatory effect via alleviating MAPKs pathways in LPS-challenged macrophage RAW264.7 cells [25]. Nevertheless, it is no well-known whether Q3G exerts protective activity *in vitro* and *in vivo* models of pulmonary injury. Thus, using models of human lung fibroblasts MRC-5 exposed to LPS and the LPS in combination with elastase (LPS/E)-induced mice experiment, the aim of the study is to investigate (i) whether Q3G has inhibitory effects on the LPS-induced cell survival loss, ROS generation, and inflammation; (ii) the role of Q3G in regulating TLR4/NF-κB signaling, NLRP3 inflammasome, pyroptotic and apoptotic cell death; and (iii) the *in vitro* and *in vivo* protective effects of Q3G against pulmonary injury.

2. Materials and methods

2.1. Cell culture and treatment

Human lung fibroblast cells MRC-5 purchased from the Bioresource Collection and Research Center (BCRC, Food Industry Research and Development Institute, Hsinchu, Taiwan) were cultured in

Minimal Essential Medium with Earle's (MEM) supplemented with 2.2 g/L sodium bicarbonate ($NaHCO_3$), 10% fetal bovine serum (FBS), 1% L-glutamine, 1% sodium pyruvate, 1% non-essential amino acids and 1% penicillin-streptomycin in a humidified incubator at 37 °C with 5% carbon dioxide (CO_2). Before treatments, MRC-5 cells were starved in MEM without FBS for 24 h. Afterwards, MRC-5 cells were pre-treated with or without Q3G (0.125 μM or 0.25 μM), Dex (10 μM) [26], or solvent dimethyl sulfoxide (DMSO, 0.125%), served as solvent control, for 6 h, and then co-incubated with LPS (10 μg/mL) for another 24 h. For the preparations of LPS, Q3G and Dex, by dissolving the powder of LPS from Sigma–Aldrich (St Louis, MO, USA) in sterilized water, LPS at the stock concentration (10 mg/mL) was prepared. Q3G (CAS no. 22688-79-5; purity >98.0%) was obtained from ChemFaces (Wuhan, Hubei, China) and prepared the stock concentration (200 μM) by dissolving the powder in DMSO. Dex, purchased from Sigma–Aldrich (St Louis, MO, USA), was prepared the stock concentration (5 mM) by dissolving the powder in 50% (v/v) ethanol.

2.2. Cell viability assay

To evaluate cytotoxicity of LPS, MRC-5 cells were seeded at a density of 6×10^4 cells/mL in a 6-well plate, and incubated with LPS at various concentrations (0, 0.5, 1, 5, 10 and 20 μg/mL) for 6, 24 and 48 h. In addition, the cell systems cytotoxicity assessment based on the rules of ISO 10993-5:2009 [27] was performed to test for *in vitro* cytotoxicity of Q3G alone. MRC-5 cells were treated with or without Q3G at various doses (from 0.0025 to 25 μM) for 24 h. The cell culture and treatment conditions were shown in Table S1. In another experiment, MRC-5 cells were pre-treated with or without Q3G (0.125 μM or 0.25 μM), or Dex (10 μM) for 6 h, and then co-incubated with LPS (10 μg/mL) for another 24 h. Briefly, after a 24-h treatment, the cells were harvested, centrifuged at 1200 rpm for 5 min and washed once with 1X sterilized phosphate buffered saline (PBS). The harvested cells were stained with 10 μg/mL of propidium iodide (PI), purchased from Sigma–Aldrich (St. Louis, MO, USA), at, and the cell viability was measured by Muse™ Cell Analyzer (EMD Millipore Corporation, Merck Life Sciences, KGaA, Darmstadt, Germany).

2.3. Reactive oxygen species (ROS) content analysis

The cellular ROS level was assayed by Muse® Oxidative Stress Kit (Luminex, Austin, TX, USA). The treated cells were incubated and stained with dichlorofluorescein diacetate (DCFH-DA). After a 24-h incubation, the fluorescence intensity of ROS generation was analyzed by the Muse™ Cell Analyzer. The values in each group were represented relative to the control, was set to be 100%.

2.4. Pro-inflammatory cytokines content analysis

After the treatments, the cell culture medium was collected. The levels of IL-1β, IL-6 and TNF-α in the medium from each groups were detected by enzyme-linked immunosorbent assay (ELISA) using ELISA MAX™ Deluxe Sets IL-1β, IL-6 and TNF-α (BioLegend, San Diego, CA, USA) according to the operation manual of datasheet.

2.5. Western blotting (WB)

After the treatments, the cell lysate was collected and extracted protein sample by radioimmunoprecipitation assay (RIPA) buffer and protease inhibitors. For the *in vivo* WB experiment, the lung tissues were randomly collected to homogenize and then assess. The protein concentrations were quantified by Dual-Range™ BCA Protein Assay Kit (Energenesis Biomedical Co., LTD, Taipei city, Taiwan). 50 μg of purified protein sample was prepared and separated by 8–15% gels of sodium dodecyl sulfate-polyacrylamide gel electrophoresis (SDS-PAGE), and then protein signals were transferred from the gel to nitrocellulose membranes (Millipore, Bedford, MA, USA). To block the non-specific binding, 5% non-fat milk was reacted with the membranes for 1 h at 4 °C. The membranes were further incubated overnight at 4 °C shaker with diluted primary antibodies against TLR4 (sc-10741), NF-κB (sc-8008), ASC (sc-514414), IL-1β (sc-12742), GSDMD (sc-81868), caspase-3 (sc-7148), caspase-8 (sc-7890), caspase-9 (sc-7885), PARP-1 (sc-56196), Bax (sc-493) and Bcl-2 (sc-7382) were purchased from Santa Cruz Biotechnology (Santa Cruz, CA, USA), NLRP3 (A12694) and IL-18 (A16737) were purchased from Abclonal (Woburn, MA, USA), and anti-β-actin (A5441) from Sigma–Aldrich (St. Louis, MO, USA). Next day, the membranes were washed with tris-buffered saline containing 0.1% Tween-20 (TBST) three times (for 10 min each time) at room temperature, then incubated 1 h at 4 °C shaker with diluted secondary antibodies anti-mouse IgG (A9044) and anti-rabbit IgG (A0545) from Sigma–Aldrich (St. Louis, MO, USA). After 1-h incubation, the membranes were rinsed three times and detected by enhanced chemiluminescence (ECL) reagent (Millipore, Burlington, MA, USA) in a

LAS-4000 Luminescent Image Analyzer (Fujifilm Corporation, Tokyo, Japan).

2.6. Apoptosis analysis

2.6.1. 4',6-diamidino-2-phenylindole (DAPI) single staining

The cell morphology change of apoptotic characteristics was detected by fluorescence microscopy. After the treatments, the monolayer of cells rinsed with PBS and fixed in 4% paraformaldehyde at room temperature for 30 min. The fixed cells were permeabilized with 0.1% Triton X-100 for 15 min and stained with 1 μg/mL of DAPI (Sigma–Aldrich, St. Louis, MO, USA) solution for 10 min. After washing with PBS for three times, the apoptotic cells were observed under 100x and 200x magnification using fluorescence microscopy. Apoptotic values were calculated as the percentage of DAPI-positive cells relative to the total number of cells in each random field, and at least 100 cells were counted for each experiment.

2.6.2. Annexin V/7-amino-actinomycin D (7-AAD) double staining

The total apoptotic cells were detected by Muse® Annexin V & Dead Cell kit (Luminex, Austin, TX, USA). The treated cells were wash for three times and resuspended in PBS, and then 100 μL of Muse™ Annexin V & Dead Cell Reagent was added to 100 μL of cell suspension. The cells were incubated for 20 min at room temperature in dark and analyzed by Muse™ Cell Analyzer.

2.7. Mitochondria membrane-potential assay

Mitochondrial membrane-potential was assayed utilizing a lipophilic cationic dye 5,5′,6,6′-tetrachloro-1,1′,3,3′-tetraethylbenzimidazolyl-carbocyanine iodide (JC-1) as described previously [28]. After the treatments, the cells planted in a 6-well plate were washed with PBS for three times, and incubated with JC-1 dye at room temperature for 10 min in dark. The JC-1-stained cells were resuspended in PBS and detected by Muse™ Cell Analyzer. Mitochondrial depolarization was quantified in the fluorescence intensity of JC-1 red/green ratio.

2.8. Multicaspase assay

To analyze apoptosis via activation of multiple caspases (caspase-1, -3, -4, -5, -6, -7, -8 and -9), the Muse™ Multicaspase assay kit (EMD Millipore Corporation, Merck Life Sciences, KGaA, Darmstadt, Germany) was performed. After the treatments, the cells were resuspended in 1x Caspase Buffer. 50 μL of cells were incubated with 5 μL of Muse™ MultiCaspase working solution at 37 °C for 30 min, and then added 150 μL of Muse™ Caspase 7-AAD working solution at room temperature for 5 min. The multicaspase activity were assayed by Muse™ Cell Analyzer and calculated as the percentage of the total caspase.

2.9. Animal experiments

Six-week-old male C57BL/6 mice were obtained from BioLASCO Taiwan Co., Ltd. (Taipei, Taiwan). Mice were housed in a controlled room with temperature at 25 ± 1 °C, relative humidity at 55 ± 2%, and a 12 h light/dark cycle. The *in vivo* experiment procedure was conducted according to the guidelines of the Institutional Animal Care and Use Committee of Chung Shan Medical University animal care committee. All mice were given Laboratory Autoclavable Rodent Diet 5010 (LabDiet, St. Louis, MO, USA) as a regular standard diet. According to the manufacturer's specifications, this standard diet contains 28.7% protein, 13.1% fat and 58.2% carbohydrates. For each mouse weighing between 20 and 25 g, the food intake approximately 20% of body weight per day, that equivalent to 4–5 g/mouse/day. After adaptation for one week, all mice were randomly divided into the following five groups: (I) control, (II) the combination of LPS and elastase (LPS/E), (III) LPS/E + Q3G (0.15 μmol/mouse), (IV) LPS/E + Dex (1 mg/kg), and (V) Q3G alone. Except for the mice of group I and V treated with PBS, the mice of group II-IV were exposed intranasally (in.) to a mixture of 7 mg LPS and 1.2 U porcine pancreatic elastase, as LPS/E challenge, in a total volume of 40 μL, and in. once per ten days for 30 days [29]. At the same time, the mice of groups III were further administrated 100 μL of Q3G at 0.15 μmol/mouse, is equivalent to 1.5 mM (approximately 3 mg/kg bw.), by oral gavage daily for 30 days [30], while the mice groups IV were received intraperitoneally (ip.) Dex, purchased from Sigma–Aldrich (St Louis, MO, USA), once per week for four consecutive weeks [31]. The administration and doses for the treatments were based on the previous studies. Body weight (bw.) of mice in each groups were recorded every 10 days (on Day 0, 10, 20, 30). Also, the growth rate of bw. was further calculated utilizing the following formulae: growth rate (%) = bw. on Day 10 − bw. on Day 1/bw. on Day 1 × 100% [32]. In accordance with a previously studied procedure [33], the mice were sacrificed by cervical dislocation. Immediately after sacrifice, the tissues of lung were surgically exposed and blood

were collected. After blood samples were centrifuged at 3000 rpm for 30 min at 4 °C to obtain serum, the serum samples were used to determine the levels of the biochemical parameters, including aspartate aminotransferase (AST), alanine aminotransferase (ALT), blood urea nitrogen (BUN) and fasting plasma glucose (FPS). The lung tissue homogenate was used for above-mentioned inflammatory cytokines assay, myeloperoxidase (MPO) activity measured by MPO activity assay kit (Bio-Vision Inc., Milpitas, CA, USA), and Western blotting.

2.10. Pulmonary function assessments

During the treatments, the pulmonary function in mice from each groups were measured four times (on Day 0, 10, 20, 30). The mice were anesthetized with 2% isoflurane (Panion & Bf Biotech Inc., Taipei, Taiwan) according to the instruction of National Laboratory Animal Center (Taipei, Taiwan) and were fixed on Rodent Surgical Monitor^{+} (Indus Instruments, Webster, TX, USA). The pulmonary function parameters, including respiratory frequency, respiratory rate, heart rate and peripheral oxygen saturation (SpO_2), were recorded by using the analytical instrument mentioned above. The respiratory frequency was captured within 0.5 s, while the respiratory rate, heart rate and SpO_2 were calculated as the mean values in 1 min.

2.11. Wet-to-dry (W/D) ratio of lung tissues

The middle lobe of the right lung was harvested and dried surface moisture with a filter paper before measuring the wet weight. Subsequently, the wet lungs were placed in the oven at 80 °C for 48 h to obtain the dry weight. The W/D ratio was further calculated for evaluation of lung edema.

2.12. Histopathology assessment of lung tissues

2.12.1. Hematoxylin and eosin (H&E) staining

The tissues of upper right lung lobe were fixed in 10% paraformaldehyde containing 10% v/v methanol for 24 h. After fixation, the lung tissues were dehydrated and embedded in paraffin. The tissues were sectioned at a thickness of 5 μm for H&E staining to assess the histopathological changes. The stained sections were observed under 200x magnification using a light microscope. Pulmonary emphysema was quantified using Image J software by measuring the mean linear intercept (MLI) [MLI = total lengths (L)/the numbers of inter-alveolar septum (Ns)] for airspace enlargement. Also, the destructive index (DI) is the ratio of damaged (D) to normal (N) tissue in the alveoli/duct space for detection of destruction of alveolar walls as previously published studies [34,35].

2.12.2. Terminal deoxynucleotidyl transferase dUTP nick end labeling (TUNEL) assay

To determine tissue apoptosis, the lung sections were analyzed by using ApoBrdU-IHC DNA Fragmentation Assay kit (BioVision Inc., Milpitas, CA, USA) according to the manufacturer's instructions. The tissues of upper right lung lobe in the different groups were taken out and fixed by 10% paraformaldehyde containing 10% v/v methanol for 24 h. After fixation, the lung tissues were dehydrated and embedded in paraffin. The tissues were sectioned at a thickness of 5 μm for the TUNEL assay. The stained sections were photographed under a light microscope at 400x magnification. The TUNEL-positive cells were calculated as the percentage of total cells at least three random fields, as published study [36].

2.13. Statistical analysis

Three or more separate experiments were performed. Data were reported as means ± standard deviation (SD) of three independent experiments. Student's *t*-test was used for the analysis between two groups with only one factor involved. For the experiments of dose response of LPS or Q3G, one-way ANOVA with post-hoc Dunnett's test was used to calculate the p value for each dose treatment compared to the untreated control (without LPS or Q3G). Regression was used to test the p value of the dependency of a parameter to dosage. Significant differences were established at $p < 0.05$.

3. Results

3.1. Dose-response and time-screening effect of LPS on cell viability in MRC-5 cells

To investigate the dose-response and time-screening effect of LPS on MRC-5 cell viability *in vitro*, LPS's cytotoxicity was measured by the morphologic observation (Fig. 1A) and Muse™ Cell Analyzer with PI stain (Fig. 1B). MRC-5 cells were treated with various concentrations of LPS (0, 0.5, 1, 5, 10 and 20 μg/mL) for 6, 24 and 48 h. The results showed that there was the harmful effect of LPS on the cell morphology and growth in a dose- but not time-dependent manner (Fig. 1C). Compared with control group, it was found the concentration of a 24 h-incubation of LPS on the inhibition of 10 percent

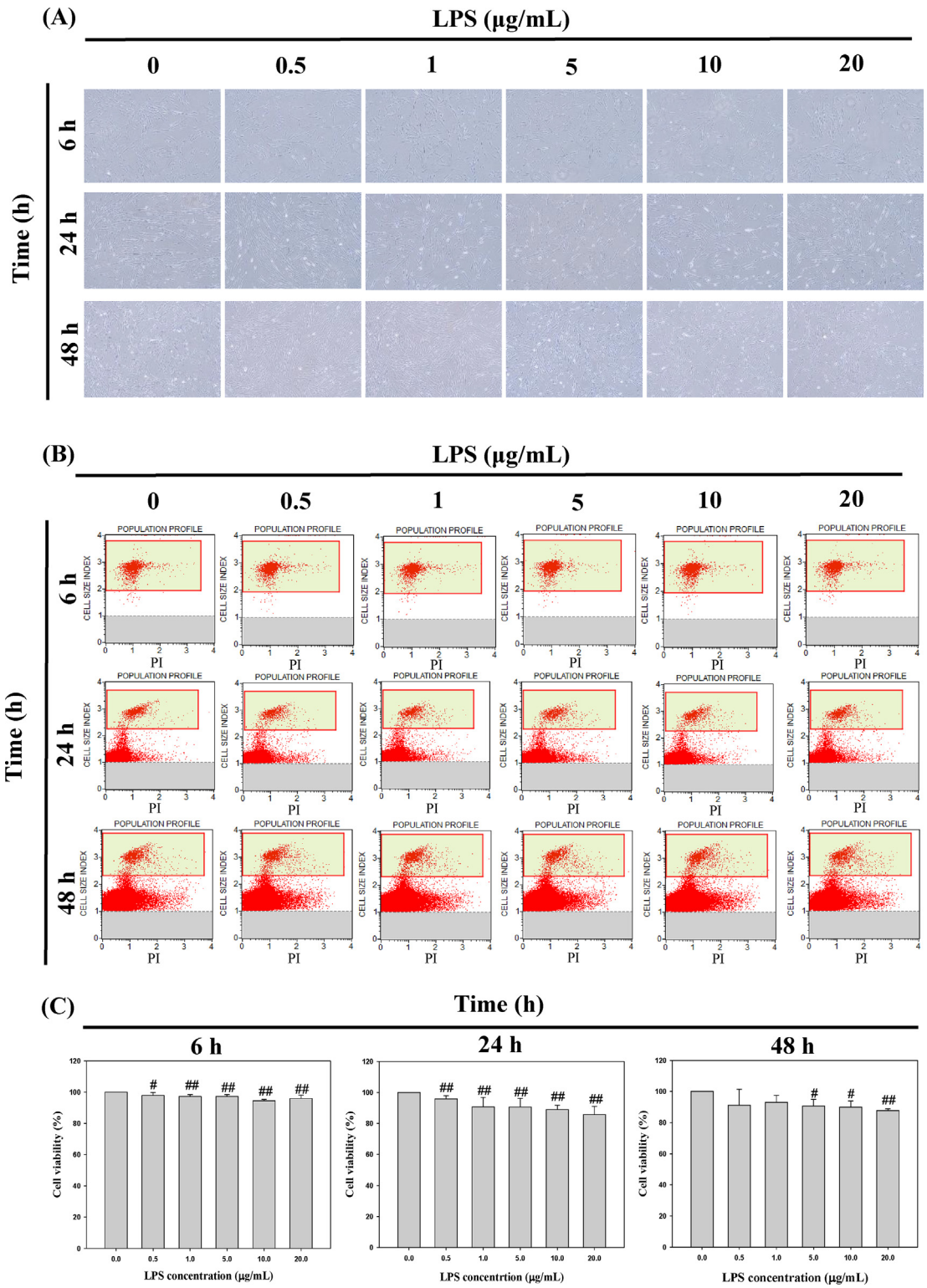

*Fig. 1. **Dose–response and time-screening effect of LPS on cell viability in MRC-5 cells.** **(A)** Representative photomicrographs of MRC-5 cells were treated with various concentrations of LPS (0, 0.5, 1, 5, 10 and 20 μg/mL) for 6, 24 and 48 h (100x). **(B)** The cell viability was measured by Muse™ Cell Analyzer with PI stain. **(C)** The quantitative data were presented as mean ± SD ($n = 3$) from three independent experiments. $^{\#}p < 0.05$, $^{\#\#}p < 0.01$ compared with the control group via one-way ANOVA with post-hoc Dunnett's test.*

(IC_{10}) of the cell survival was about 10 μg/mL (Fig. 1C). According to the consideration mentioned above and previous reports [37], this dose was applied in all subsequent experiments to explore the influences of cell growth, inflammation, and apoptosis.

3.2. Effects of Q3G on the LPS-induced cell survival loss and cellular ROS generation in MRC-5 cells

Referred on previous studies [25], we first have tested the dose-screening effect of Q3G at various doses (from 0.0025 to 25 μM) on MRC-5 cell viability *in vitro*. According to the rules of ISO 10993-5:2009 [27], the Q3G's cytotoxicity was evaluated and further measured by the morphologic observation and Muse™ Cell Analyzer with PI stain (Fig. S1). The qualitative and quantitative assessments were conducted. For the qualitative evaluation for *in vitro* cytotoxicity of Q3G, not more than 20% of the cells were loosely attached and showed changes in morphology upon the dose higher than 0.25 μM (Fig. S1A). It might be estimated in grade 1 (slight) on the basis of qualitative morphological grading of cytotoxicity based on Table S2. For the quantitative evaluation, Fig. S1B showed that Q3G at 0.0025−0.25 μM was nontoxic for MRC-5 cells, while Q3G decreased the cell viability at the dose higher than 0.25 μM. Hence, the two doses, 0.125 and 0.25 μM, were selected as low or high concentrations of Q3G for further mechanistic studies.

To explore the effect of Q3G on the LPS-induced cell survival loss, oxidative stress and apoptosis, MRC-5 cells were pre-treated with or without Q3G (0.125 μM or 0.25 μM) or DMSO, served as solvent control, for 6 h, and then co-incubated with LPS (10 μg/mL) for another 24 h. MRC-5 cells either untreated (control cells) or exposed to DMSO (solvent control) did not have any microscopically discernible adverse effects (*panel 1*, Fig. 2A), and the effect of DMSO on cell viability (*panel 2*, Fig. 2A and B), and ROS content (*panel 3*, Fig. 2A and C) exhibited no significant differences, comparing to the control group, implying to exclude the effect of the solvent DMSO on this study. Using Muse™ Cell Analyzer, the quantitative data of cell viability assay showed that either low or high doses of Q3G significantly rescued MRC-5 cell injury caused by LPS (Fig. 2B). In addition, Q3G at these doses also markedly decreased the cellular ROS generation in a dose-dependent manner (Fig. 2C). It is worth noting the combination of LPS and Q3G demonstrated significant antagonistic efficacy, especially at the dose of 0.25 μM for Q3G, under which the LPS-mediated inhibition of cell growth and induction of ROS generation was almost completely blocked (Fig. 2B and C). Collectively, in the presence of LPS, Q3G has the effects in not only protecting the cell viability, but also inhibiting the ROS production in MRC-5 cells.

3.3. Effects of Q3G on the LPS-induced inflammation reaction and NLRP3 inflammasome activation in MRC-5 cells

To further investigate the inhibitory effect of Q3G at 0.25 μM on the LPS-induced inflammation in MRC-5 cells, the levels of pro-inflammatory cytokines, including IL-1β, IL-6 and TNF-α, in the culture medium of treatments cells were detected by ELISA assays. The results revealed that there were significant increases in the contents of above-mentioned cytokines induced by LPS, especially in that of IL-1β, were abrogated by Q3G (Fig. 3A). In order to clarify the mechanisms by which Q3G modulates LPS-mediated cell survival loss and IL-1β production in MRC-5 cells, the effect of Q3G on TLR4/NF-κB signaling and NLRP3 inflammasome activation was investigated. As shown in Fig. 3B, Western blot analysis showed that protein levels of TLR4 and NF-κB were decreased in the cells pre-incubated with Q3G, comparing to LPS alone. Fig. 3C indicated the LPS stimulation increased the protein levels of NLRP3, ASC, active-caspase-1 and mature-IL-1β, which are considered hallmarks of NLRP3 inflammasome activation. Pre-treatment with Q3G significantly prevented expression of NLRP3, speck formation of ASC, activation of caspase-1 and maturation of IL-1β by LPS (Fig. 3C). In parallel, Q3G also inhibited the LPS-induced increases in levels of IL-18 and GSDMD, both are critical for pyroptotic cell death, in MRC-5 cells (Fig. 3D). Therefore, the results suggested that Q3G suppressed the cell inflammation and NLRP3 inflammasome activation, leading to the inhibition of pyroptosis that occurred in the LPS-treated MCR-5 cells.

3.4. Effects of Q3G on the LPS-induced apoptosis in MRC-5 cells

For evaluating whether the protective effect of Q3G against LPS from cell survival loss may be involved with anti-apoptosis, a series of apoptosis-related analysis was conducted. First, the morphological features of apoptosis, including cell shrinkage, nuclear condensation and fragmentation, induced by LPS were explored using DAPI single staining (*panels 1-4*, Fig. 4A). Comparing to LPS group, pre-treatment with the high dose of Q3G

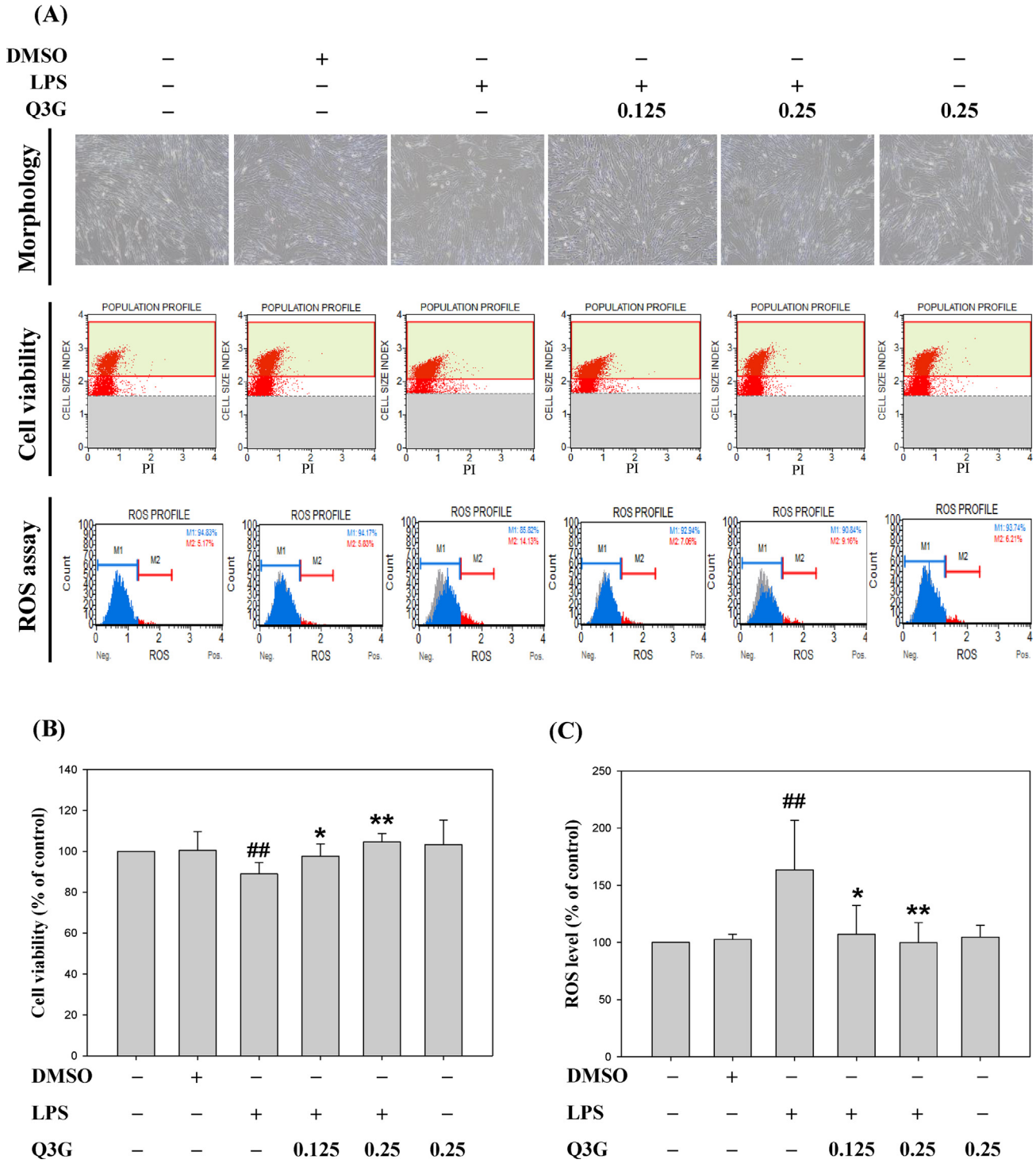

*Fig. 2. **Effects of Q3G on the LPS-induced cell survival loss and ROS generation in MRC-5 cells.** **(A)** Representative photomicrographs of MRC-5 cells were pre-treated with or without Q3G (0.125 or 0.25 μM) or DMSO (0.125%) for 6 h, and then co-incubated with LPS (10 μg/mL) for another 24 h (200x, upper panel). The cell viability was measured by Muse™ Cell Analyzer (middle panel). The ROS were assayed by Oxidative stress kit with Muse™ Cell Analyzer (lower panel). The quantitative data of cell viability **(B)** and ROS content **(C)** were presented as mean ± SD (n = 3) from three independent experiments. ##p < 0.01 compared with the control group via student's t-test. *p < 0.05, **p < 0.01 compared with the LPS group via student's t-test.*

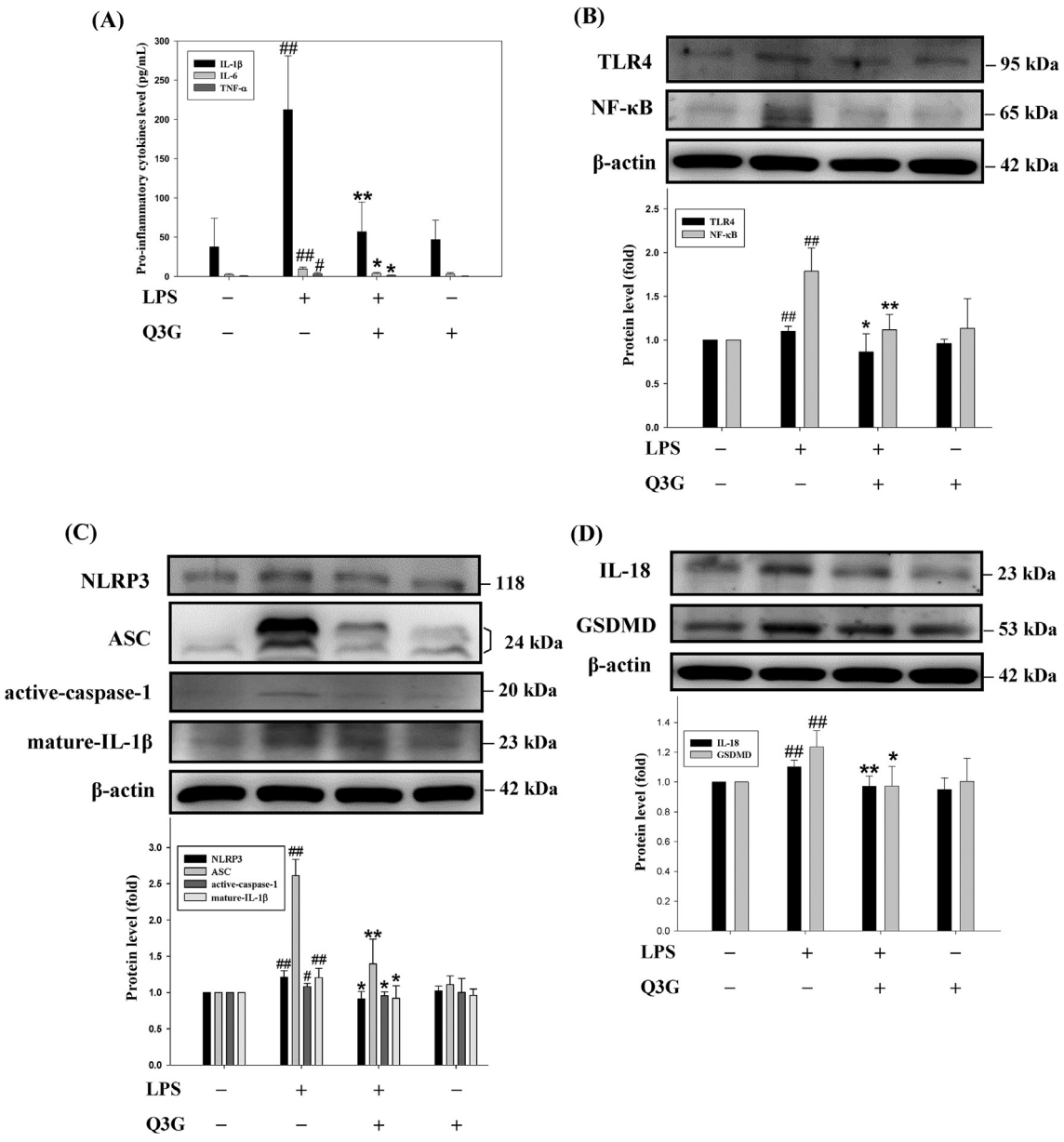

Fig. 3. ***Effects of Q3G on the LPS-induced inflammation, inflammasome activation and pyroptosis in MRC-5 cells.*** *MRC-5 cells were pre-treated with or without Q3G (0.25 μM) for 6 h, and then co-incubated with LPS (10 μg/mL) for another 24 h.* ***(A)*** *The levels of inflammatory cytokines, including IL-1β, IL-6 and TNF-α, in the culture medium of treatments cells, were detected by ELISA assays. The protein levels of TLR4, NF-κB* ***(B)****, NLRP3, ASC, active-caspase-1, mature-IL-1β* ***(C)****, IL-18 and GSDMD* ***(D)*** *were analyzed by Western blotting. β-actin was served as an internal control. The quantitative data were presented as mean ± SD (n = 3) from three independent experiments.* $^{\#}p < 0.05$, $^{\#\#}p < 0.01$ *compared with the control group via student's t-test.* $^{*}p < 0.05$, $^{**}p < 0.01$ *compared with the LPS group via student's t-test.*

(0.25 μM) significantly decreased the proportion of DAPI-positive cells, as shown in Fig. 4B. Furthermore, Muse™ Cell Analyzer was performed to examine the total apoptosis, combined early and late apoptosis fractions, using annexin V/7-AAD double staining (*panel 5*, Fig. 4A), and the quantitative data confirmed that Q3G exerted an inhibitory effect on the LPS-induced the increases of total apoptotic cells, which appeared in similar variation tendency to DAPI staining (Fig. 4C). In addition, the low dose of Q3G (0.125 μM) showed the capability to reduce the LPS-induced occurrence of apoptosis, similar to the results of cell viability and ROS assays, as shown in Fig. S2.

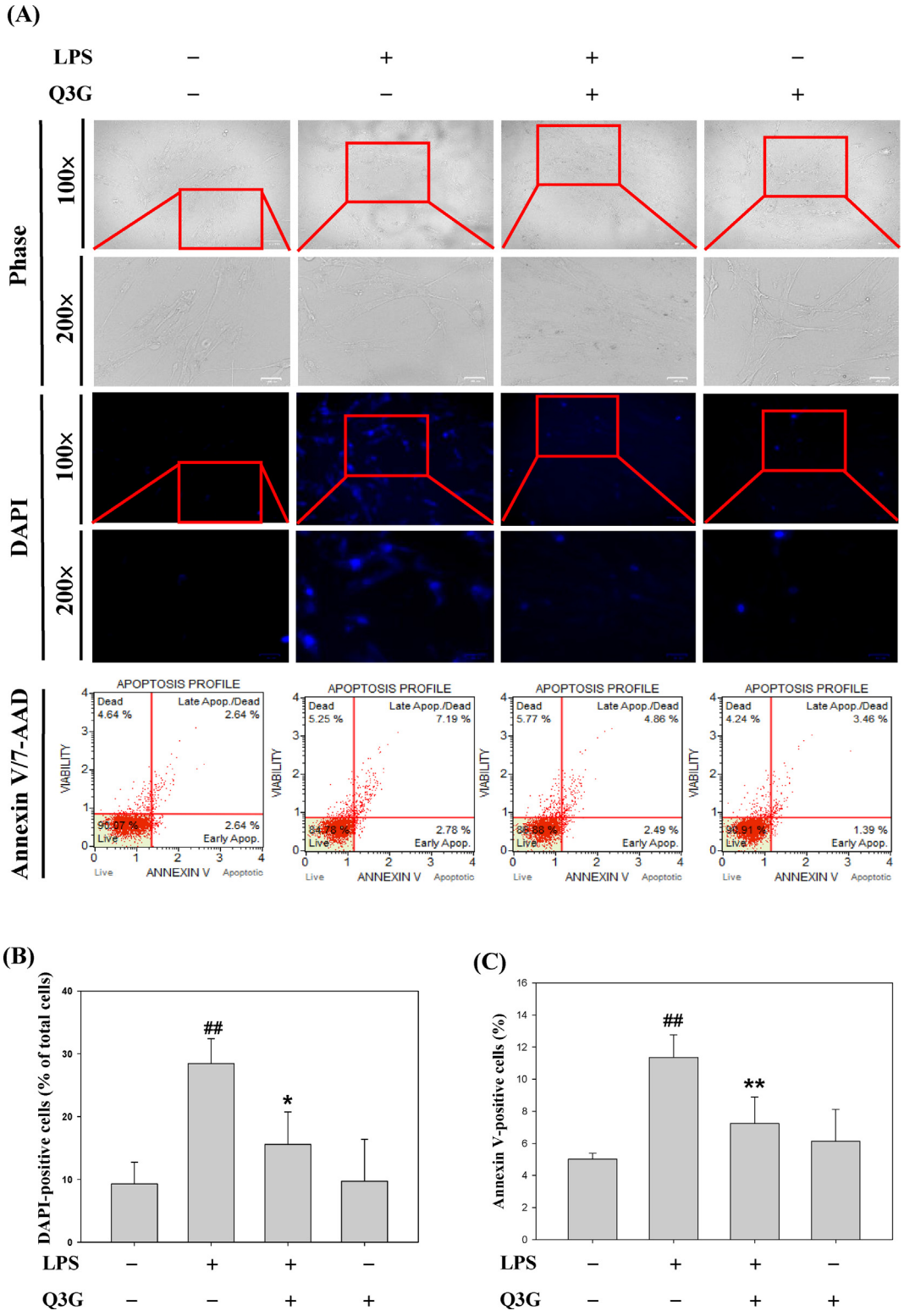

Fig. 4. ***Effects of Q3G on the LPS-induced cell apoptosis in MRC-5 cells.*** *MRC-5 cells were pre-treated with or without Q3G (0.25 μM) for 6 h, and then co-incubated with LPS (10 μg/mL) for another 24 h.* ***(A)*** *Photomicrographs of MRC-5 cells showed phase-contrast and DAPI staining (100x and 200x, panels 1-4). The annexin V/7-AAD was measured by Muse™ Cell Analyzer (panel 5).* ***(B)*** *Apoptotic values were calculated as the percentage of DAPI-positive cells relative to the total number of cells in each random field (>100 cells).* ***(C)*** *Muse™ Cell Analyzer assay of plasma membranes with annexin V/7-AAD staining, a significant number of total apoptotic cells were stained with positive annexin V-FITC and 7-AAD (right quadrant). The quantitative data were presented as mean ± SD (n = 3) from three independent experiments. $^{\#}p < 0.05$, $^{\#\#}p < 0.01$ compared with the control group via student's t-test. $^{*}p < 0.05$, $^{**}p < 0.01$ compared with the LPS group via student's t-test.*

3.5. Effects of Q3G on the LPS-mediated mitochondrial apoptotic pathway in MRC-5 cells

Mitochondria has been reported that it considerably influences apoptotic cell death, and the most significant event is the loss of mitochondrial transmembrane potential and caspase activation [38]. To determine the anti-apoptotic effect of Q3G on the LPS-treated MCR-5 cells through down-regulation of mitochondrial apoptosis pathway, the mitochondria membrane potential and caspase activity were respectively investigated using Muse™ Cell Analyzer with JC-1 staining and multicaspase assay (Fig. 5A). The JC-1 red/green fluorescence ratio can be considered as a direct assessment of the state of the mitochondria polarization [39]. During apoptosis accompanied with loss of mitochondria membrane potential, JC-1 aggregates were unable to accumulate in the mitochondria and then dissipated into JC-1 monomers, leading to the outcome of a reduction in the ratio of red to green fluorescence. As shown in Fig. 5B, the red/green ratio was remarkably decreased from 2.21 ± 0.06 (control) to 1.80 ± 0.11 after stimulation with LPS for 24 h, which was increased by the Q3G treatment. Also, LPS-induced an increase in multicaspase activity of MRC-5 cells was reversed by Q3G (Fig. 5C). Consequently, these results indicated that Q3G decreased the LPS-induced apoptosis involving mitochondrial apoptosis pathway in MRC-5 cells.

Furthermore, mechanistic assays indicated the LPS challenge for 24 h significantly induced the cleavage of caspases family, including caspase-3, -8 and -9 compared to that in the control group, which were analyzed by Western blotting. The pre-treatment with Q3G markedly reduced the LPS-induced cleavage of these caspases, especially caspase-3 p17 and p11 (Fig. 5D). The decreased protein expressions were also detected in the downstream factor of caspase-3, poly (ADP ribose) polymerase-1 (PARP-1), and its upstream factor pro-apoptotic protein Bcl-2-associated X protein (Bax), rather than anti-apoptotic protein Bcl-2 [10,11,38] in the cells co-treated with LPS and Q3G (Fig. 5E). As stated above, Q3G had the effect on inhibiting mitochondrial apoptosis pathway in the LPS-stimulated MRC-5 cells.

3.6. Effects of Q3G on the pulmonary function and physiological status in mice induced by LPS/E

To further confirm whether the *in vivo* effect of Q3G against pulmonary injury achieved similar results of *in vitro*, a mice model pulmonary injury induced by LPS/E was performed as previously established [29]. In addition to the administration of LPS/E, the mice of groups III were further were given Q3G at 0.15 μmol/mouse by oral gavage daily, referred to past studies [30]. The severity of LPS/E-induced lung injury was investigated through pulmonary function parameters, respiratory rate, heart rate and SpO_2, as well as histological findings. Comparing control group, the respiratory rates were remained unstable (Fig. 6A) and significantly decreased on Day 10 and persisted up to Day 30 (Fig. 6B) after LPS/E challenge. Simultaneously, there was a comparable tendency to heart rate in the mice of LPS/E group (Fig. 6C). Fig. 6A and B showed the pathological changes of respiratory rate and heart rate were improved from Day 10 to Day 30 after administration with Q3G, rather than Dex. In addition to respiratory rate been found to be still lower in the group of LPS/E plus Dex, the heart rate was an obvious decline on Day 10 and later was enhanced and maintained on Day 20–30 compared to that in the LPS/E group, displaying a delay improvement. Until Day 30, Q3G and Dex can significantly elevate SpO_2 reduced by LPS/E injection, while the SpO_2 in group of LPS/E plus Q3G was maintained higher than that in the group of LPS/E plus Dex (Fig. 6D). Furthermore, Fig. 6E also illustrated that LPS/E attenuated the bw. growth, and Q3G significantly raised the growth on Day 30. Altogether, Q3G can improve the respiratory rate, heart rate SpO_2 in the LPS/E-treated mice, and thereby enhanced respiratory function and bw. growth.

In the process of animal experiment, no apparent differences between control group and Q3G-treated group was observed in the serum biochemical parameters, including liver and renal functions AST, ALT and BUN (Table 1). Among serum biochemical parameters, FPS was significantly increased after LPS/E-injected mice were treated with Q3G (Table 1), confirming that Q3G has an improving-effect on physiology status of mice. Also, there is no significant change in the ratio of organ weight to body weight of mice from Q3G alone group, comparing to the control group (Table 2).

3.7. Effects of Q3G on lung edema and lung histopathology in mice induced by LPS/E

To further evaluate the effect of Q3G on lung edema in the LPS/E-induced mice, the images of lung tissues were observed, and then total lung weight, the wet and dry weights of the lungs were evaluated. The results of Fig. 7A and B found that when compared with control group, the LPS/E-treated mice exhibited the increases in gross

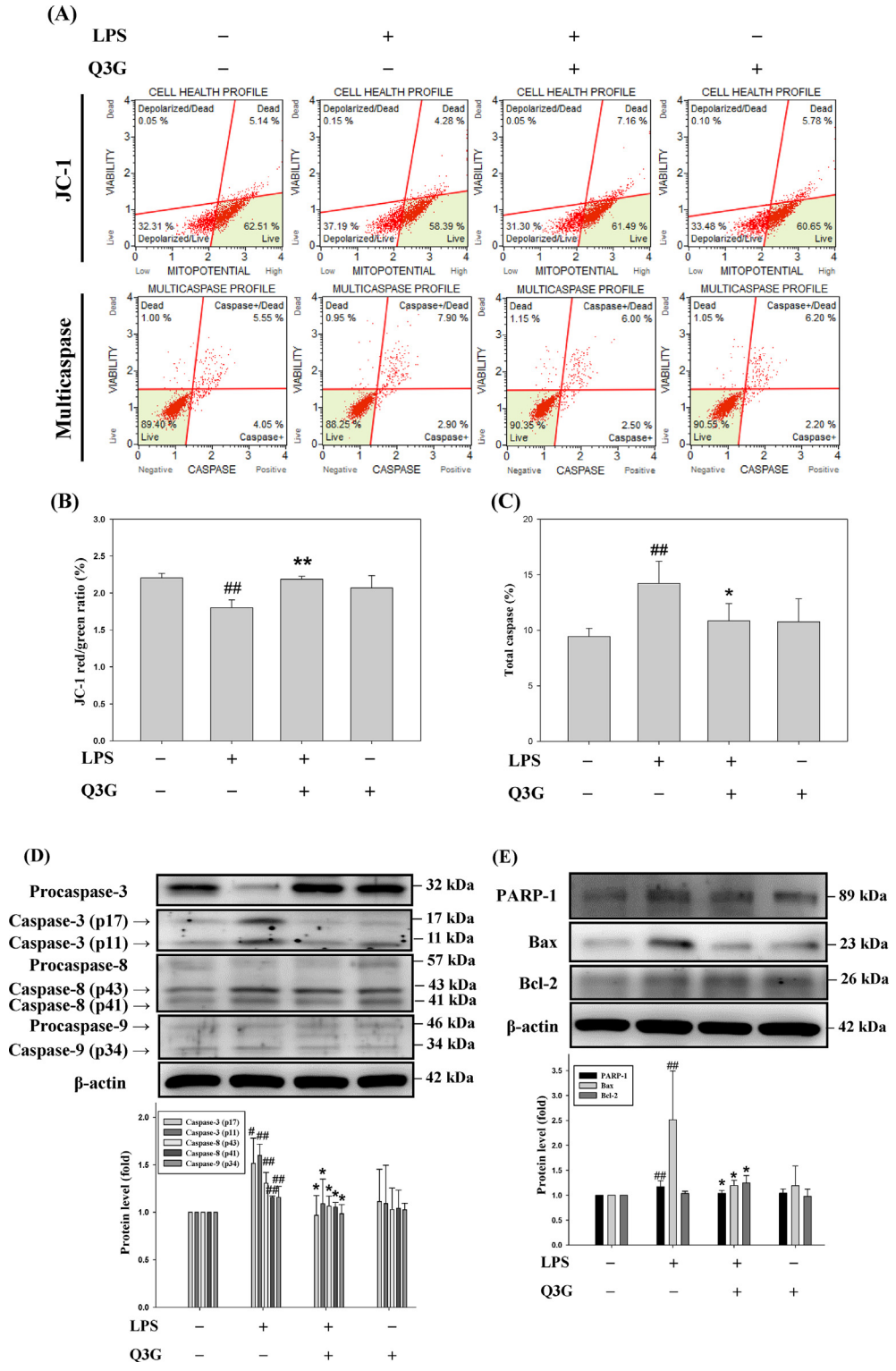

Fig. 5. ***Effects of Q3G on the LPS-induced mitochondrial apoptosis pathway in MRC-5 cells.*** *MRC-5 cells were pre-treated with or without Q3G (0.25 μM) for 6 h, and then co-incubated with LPS (10 μg/mL) for another 24 h.* ***(A)*** *The JC-1 (upper panel) and multicaspase activity (lower panel) were measured by Muse™ Cell Analyzer.* ***(B)*** *Quantitative analysis of ratio of JC-1 red/green fluorescent intensity.* ***(C)*** *The multicaspase activity was calculated as the percentage of the total caspase. The protein levels of caspase-3, caspase-8, caspase-9* ***(D)****, PARP-1, Bax and Bcl-2* ***(E)*** *were analyzed by Western blotting. β-actin was served as an internal control. The quantitative data were presented as mean ± SD (n = 3) from three independent experiments. #p < 0.05, ##p < 0.01 compared with the control group via student's t-test. *p < 0.05, **p < 0.01 compared with the LPS group via student's t-test.*

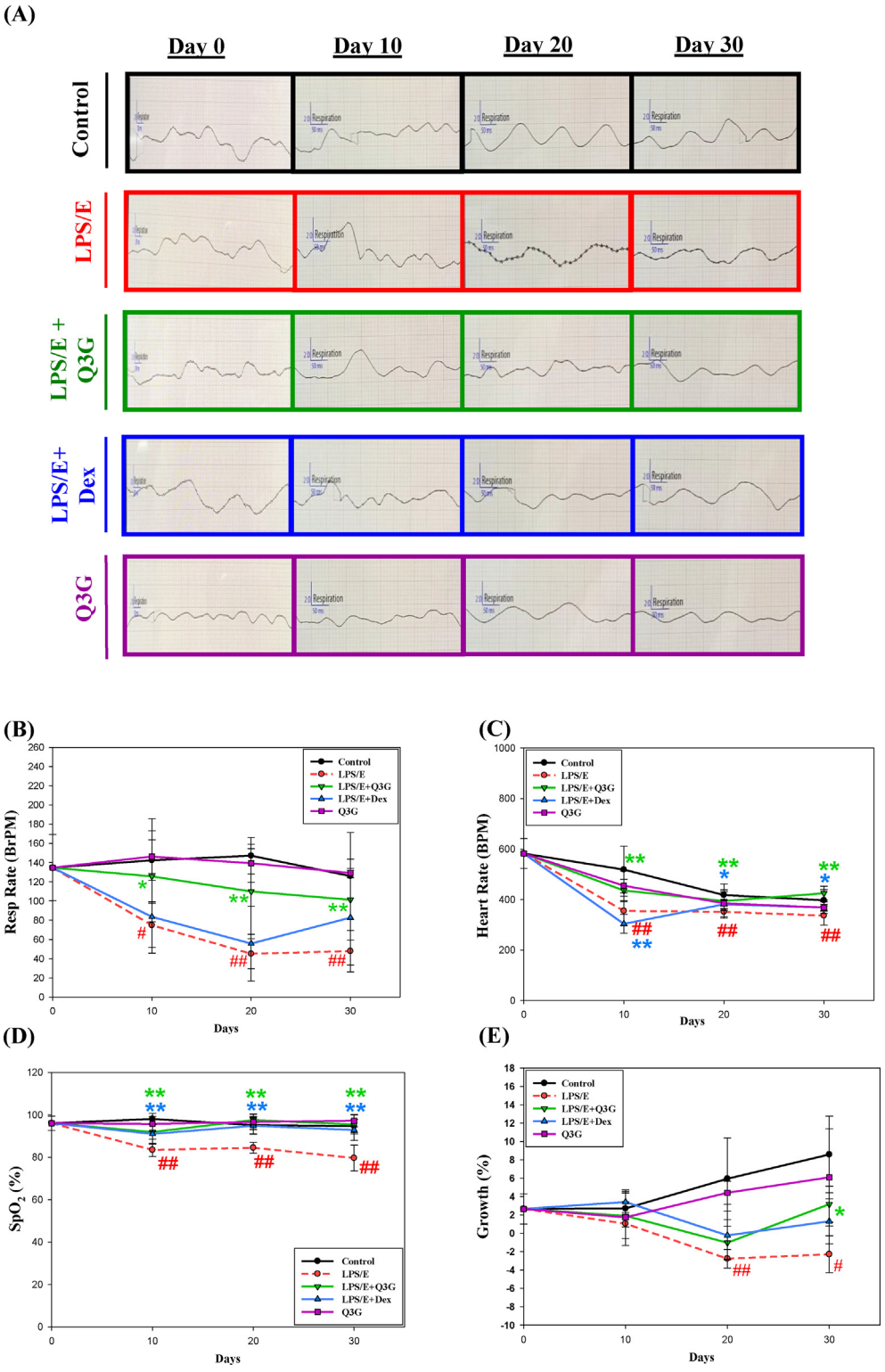

Fig. 6. ***Effects of Q3G on pulmonary function and physiologic statues in mice induced by LPS/E.*** *The C57BL/6 mice were treated with or without Q3G (0.15 μmol/mouse) daily or Dex (1 mg/kg, i.p.) once weekly in the presence or absence of LPS/E (7 μg LPS and 1.2 U elastase, i.n.) once per ten days for 30 days.* ***(A)*** *The respiratory frequency was captured within 0.5 s from Day 0 to 30 in the normal group, LPS/E-treated group, LPS/E + Q3G group, LPS/E + Dex group, and Q3G group. The respiratory rate* ***(B)****, heart rate* ***(C)****, SpO2* ***(D)*** *and the bw. growth* ***(E)*** *were measured from each group on Day 0, 10, 20, 30. The quantitative data were presented as mean ± SD (n = 6) from one independent experiment. #p < 0.05, ##p < 0.01 compared with the control group via student's t-test. *p < 0.05, **p < 0.01 compared with the LPS/E group via student's t-test.*

Table 1. Effects of Q3G on the serum biochemical parameters of mice induced by LPS/E treatment[a].

Variable[b]	Control	LPS/E	LPS/E + Q3G	LPS/E + Dex	Q3G
AST (U/L)	625.00 ± 113.14	938.00 ± 97.58	935.50 ± 224.15	799.67 ± 382.83	736.50 ± 64.35
ALT (U/L)	95.50 ± 16.26	151.6 ± 72.86	121.50 ± 37.48	83.00 ± 19.80	110.00 ± 5.66
BUN (mg/dL)	22.05 ± 0.64	23.60 ± 0.57	23.45 ± 1.48	20.20 ± 5.23	22.20 ± 0.71
FPS (mg/dL)	171.67 ± 17.47	108.75 ± 29.40[c]	158.00 ± 14.11[d]	149.33 ± 12.66	175.50 ± 12.87

[a] Values were represented as the mean ± SD (n = 6/group). Duration of the experiment = 30 days. The results were statistically analyzed with Student's *t* test.
[b] AST, aspartate aminotransferase; ALT, alanine transaminase; BUN, blood urea nitrogen; FPS, fasting plasma sugar.
[c] $p < 0.05$ compared with the control group.
[d] $p < 0.05$ compared with the LPS/E group.

appearance and the ratio of lung weight to bw., were recovered by Q3G and Dex. LPS/E significantly increased the W/D ratio of lung, meaning the characteristics of lung edema in these mice (Fig. 7C). The data also induced that Q3G markedly reduced lung W/D ratio and exerted greater effects than Dex in decreasing the degree of lung edema.

The histopathological changes in lung tissues were further analyzed by H&E staining. In LPS/E group, extensive thickening of the alveolar walls, obvious inflammatory cells infiltration and severe alveolar space destruction were observed compared to the control group. However, the histopathological deterioration was significantly alleviated by Q3G and Dex. (*upper panel*, Fig. 8A). The development of pulmonary emphysema was measured and scored by the increases in MLI and DI from the H&E stained lung tissue sections [34,35]. As shown in Fig. 8B, the representative enlargement images of H&E stain were compared from control and LPS/E group. Consistent with the histological observations, the LPS/E-induced the increases in air space enlargement (*left axis*, Fig. 8C) and destruction of alveolus (*right axis*, Fig. 8C), were attenuated by Q3G and Dex. Additionally, the data of Fig. 8A (*lower panel*) represented an obvious increase in the number of TUNEL-positive apoptotic cells in the LPS/E-treated mice when compared to those of the control group. Comparing to the LPS/E model mice, these pathological alterations of the lungs were rescued by Q3G and Dex (Fig. 8D), suggesting that Q3G possessed an anti-apoptotic effect *in vivo*. These findings concluded that Q3G improved the histological abnormalities and apoptosis lesion in the lung tissues of the LPS/E-induced mice.

3.8. Effects of Q3G on lung inflammation and the expressions of inflammatory, pyroptotic and apoptotic factors in mice induced by LPS/E

To assess the effects of Q3G on lung inflammation, the levels of pro-inflammatory cytokines and activity of MPO, a specific marker of neutrophil infiltration and inflammatory injury of the lungs [40], were detected in the lungs of LPS/E-induced mice. After LPS/E challenge, there were significant increases in levels of IL-1β, IL-6 and TNF-α (Fig. 9A), as well as MPO-1 activity (Fig. 9B). Otherwise, only Q3G, rather than Dex, decreased the inflammatory profiles in this model. Furthermore, to explore whether Q3G inhibited renal inflammation and cell death, the protein expressions of inflammatory, pyroptotic and apoptotic factors were investigated. As shown in Fig. 9C, the levels of NF-κB, IL-1β, GSDMD and caspase-3 (p17) were obviously up-regulated by LPS/E, which were decreased by Q3G and Dex treatments. Consistent with the results of *in vitro*, the *in vivo* study revealed that Q3G improved the pulmonary injury which induced by LPS/E through suppressing the inflammation, pyroptosis and apoptosis (Fig. 10).

4. Discussion

Pulmonary injury is a severe clinical condition and characterized by widespread inflammation in

Table 2. Effect of Q3G on the ratio of organ weight to bw. of mice induced by LPS/E treatment[a].

Organ weight (mg)/bw. (g)	Control	LPS/E	LPS/E + Q3G	LPS/E + Dex	Q3G
Liver	54.34 ± 3.99	51.18 ± 5.19	53.63 ± 4.50	50.43 ± 4.90	53.62 ± 3.62
Spleen	2.40 ± 0.62	3.46 ± 0.63[b]	2.44 ± 0.64[c]	2.70 ± 0.65	2.68 ± 0.37
Kidney	15.53 ± 0.42	14.16 ± 0.88[b]	15.24 ± 0.73[c]	14.96 ± 1.20	14.84 ± 0.88

[a] Values were represented as the mean ± SD (n = 6/group). Duration of the experiment = 30 days. The results were statistically analyzed with Student's *t* test.
[b] $p < 0.05$ compared with the control group.
[c] $p < 0.05$ compared with the LPS/E group.

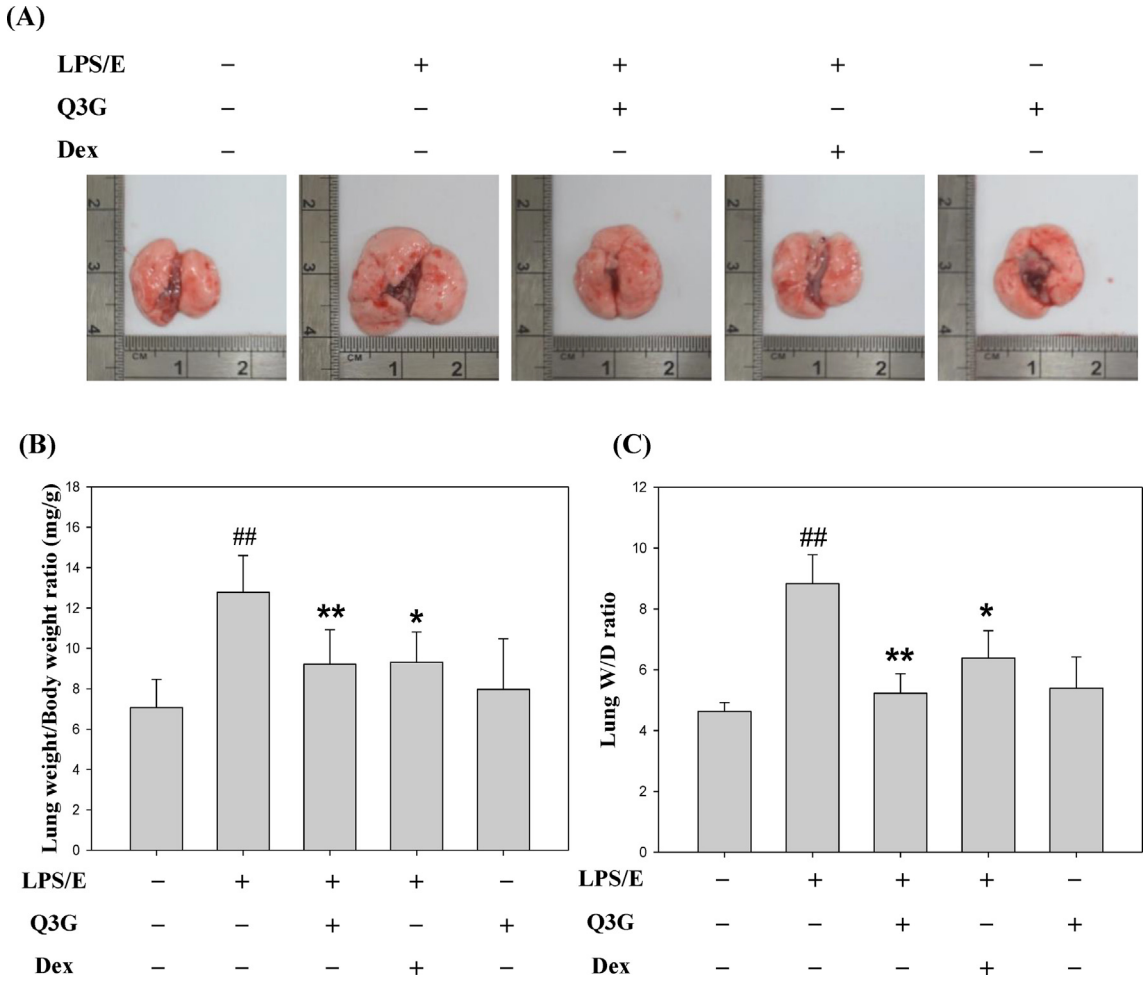

*Fig. 7. **Effects of Q3G on lung edema in C57BL/6 mice induced by LPS/E.** The C57BL/6 mice were treated with or without Q3G (0.15 μmol/mouse) daily or Dex (1 mg/kg, i.p.) once weekly in the presence or absence of LPS/E (7 μg LPS and 1.2 U elastase, i.n.) once per ten days for 30 days. **(A)** Representative photographs of the lung tissue from each group. The lung weight/bw. ratio **(B)** and lung W/D ratio **(C)** were measured after sacrificed. The quantitative data were presented as mean ± SD (n = 6) from one independent experiment. $^{\#\#}p < 0.01$ compared with the control group via student's t-test. *p < 0.05, **p < 0.01 compared with the LPS/E group via student's t-test.*

the lung. ARDS and COPD have been conducted to explore the mechanism and novel therapeutic treatments in many studies [41–43]. During the pathogenesis of these lung diseases, programmed cell death, including apoptosis, pyroptosis and autophagy, has been also demonstrated to play a pivotal role [9–11,44]. Therefore, modulating programmed cell death of lungs could be a valuable strategy for pulmonary injury, actually inhibiting and reversing this illness to an advanced degree instead of just blocking inflammation. Steroids, such as Dex, are generally used as anti-inflammatory drugs for the treatments of ARDS and COPD. However, there are severe side effects and still no effective pharmacological therapies for pulmonary injury applying these drugs [45,46]. In recent years, flavonoids, which are usually presented in vegetables, fruits, and plant-derived products, are considered as not only natural sources of antioxidants to remove ROS, but also the anti-inflammatory agents [47]. Many *in vitro* studies have shown that several natural compounds, which are rich in flavonoids, alleviate the inflammation and apoptosis on the LPS-induced lung cells [48,49]. Q3G, a kind of flavonoids found in fruits, vegetables and medicinal plants, is a major metabolite of quercetin in human plasma [13], and has been regarded as the potential agent to treat many diseases due to its various effects on anti-inflammatory, antioxidants and anti-aging [18,19,23]. In this study, we hypothesized that the bioactivity of Q3G may ameliorate the abnormalities which were caused by the LPS-stimulated pulmonary injury. To our understanding, this is the first study to investigate the protective effects of Q3G against pulmonary injury *in vitro* and *in vivo*.

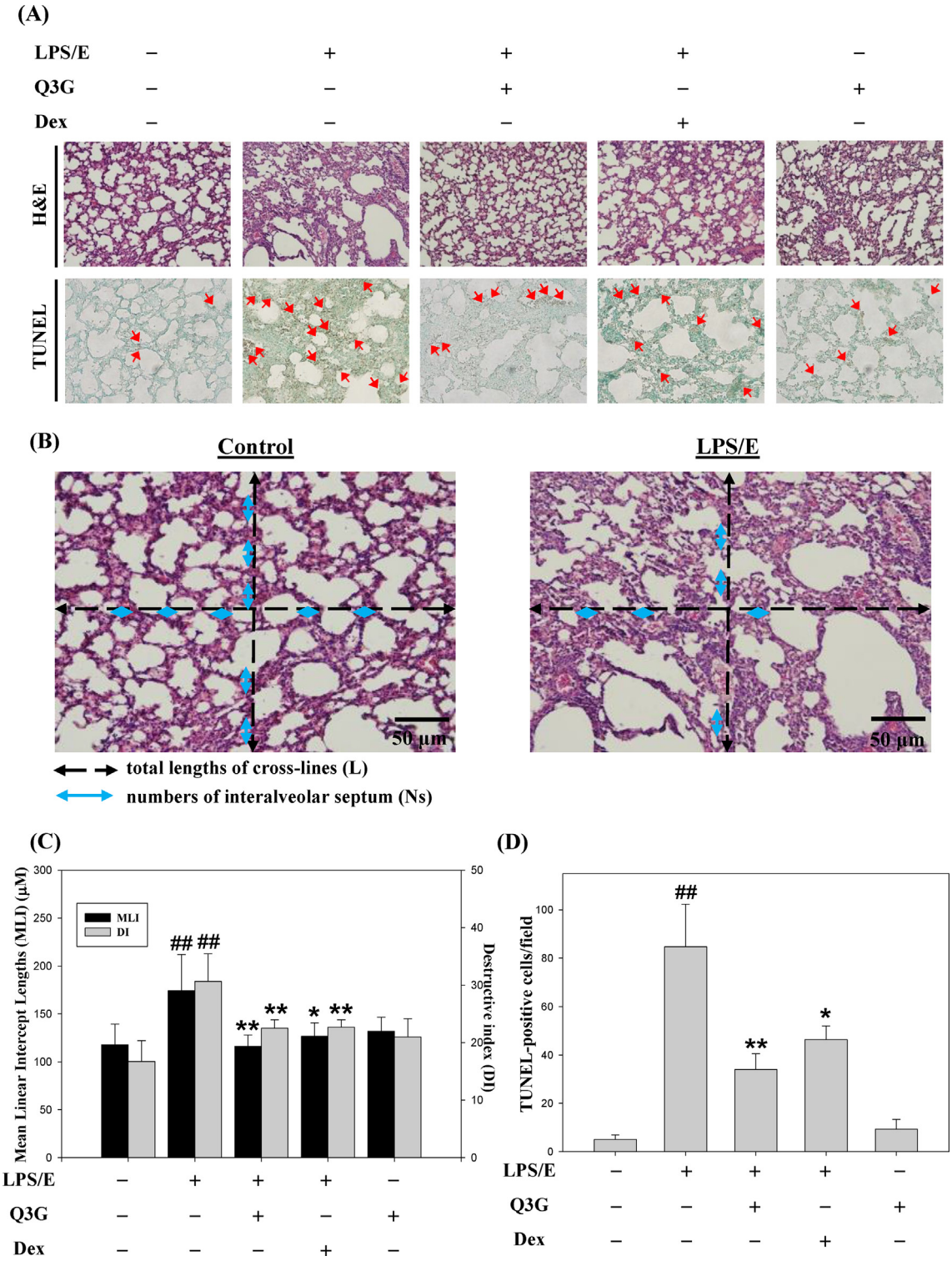

*Fig. 8. Effects of Q3G on lung histopathology in mice induced by LPS/E. The C57BL/6 mice were treated with or without Q3G (0.15 μmol/mouse) daily or Dex (1 mg/kg, i.p.) once weekly in the presence or absence of LPS/E (7 μg LPS and 1.2 U elastase, i.n.) once per ten days for 30 days. (A) Representative images of lung sections from different treatments (n = 6/group) stained with H&E (200x, upper panel) and TUNEL staining (400x, lower panel) to display the lung histological abnormalities. Red arrows indicate apoptotic cells. (B) Representative images of H&E stain (200x) from control and LPS/E group to represent the total lengths of cross-lines (L) by the black dashed lines, and the numbers of interalveolar septum (Ns) by the blue solid lines. (C) The mean linear intercept lengths (MLI, left panel) and the destructive index (DI, right panel) were scored from histological sections from each group. (D) The quantitative data of TUNEL stain were presented as mean ± SD (n = 6) from one independent experiment. ##p < 0.01 compared with the control group via student's t-test. *p < 0.05, **p < 0.01 compared with the LPS/E group via student's t-test.*

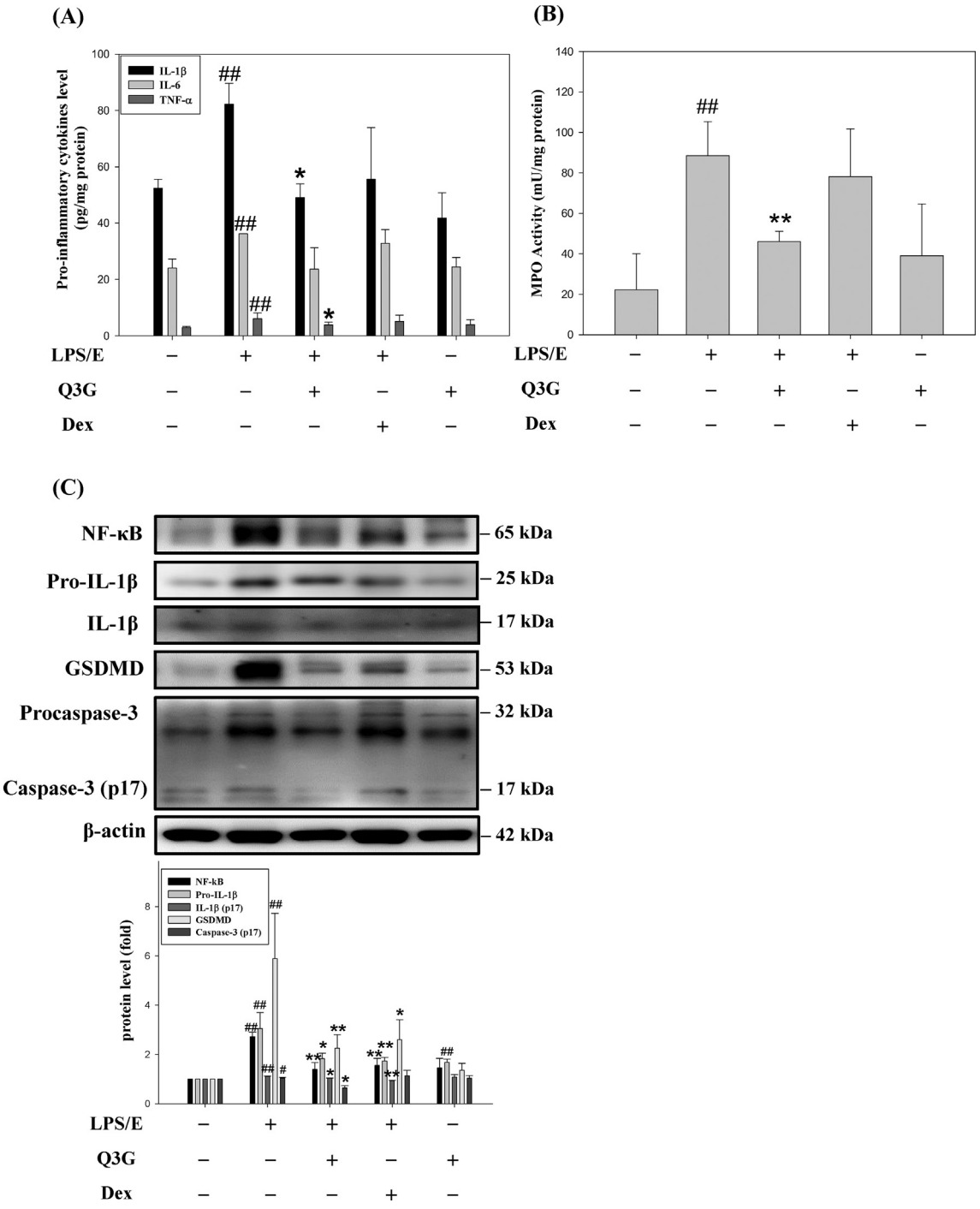

*Fig. 9. **Effects of Q3G on lung inflammation and the expressions of inflammatory, pyroptotic, apoptotic factors in mice induced by LPS/E.** The C57BL/6 mice were treated with or without Q3G (0.15 μmol/mouse) daily or Dex (1 mg/kg, i.p.) once weekly in the presence or absence of LPS/E (7 μg LPS and 1.2 U, i.n.) once per ten days for 30 days. The inflammatory cytokines, including IL-1β, IL-6 and TNF-α levels **(A)**, and MPO activity **(B)** in the lung tissue from each group were detected by ELISA assays. **(C)** The protein levels of NF-κB, IL-1β, GSDMD and caspase-3 were analyzed by Western blotting. β-actin was served as an internal control. The quantitative data were presented as mean ± SD (n = 6) from one independent experiment. $^{\#}p < 0.05$, $^{\#\#}p < 0.01$ compared with the control group via student's t-test. $^{*}p < 0.05$, $^{**}p < 0.01$ compared with the LPS/E group via student's t-test.*

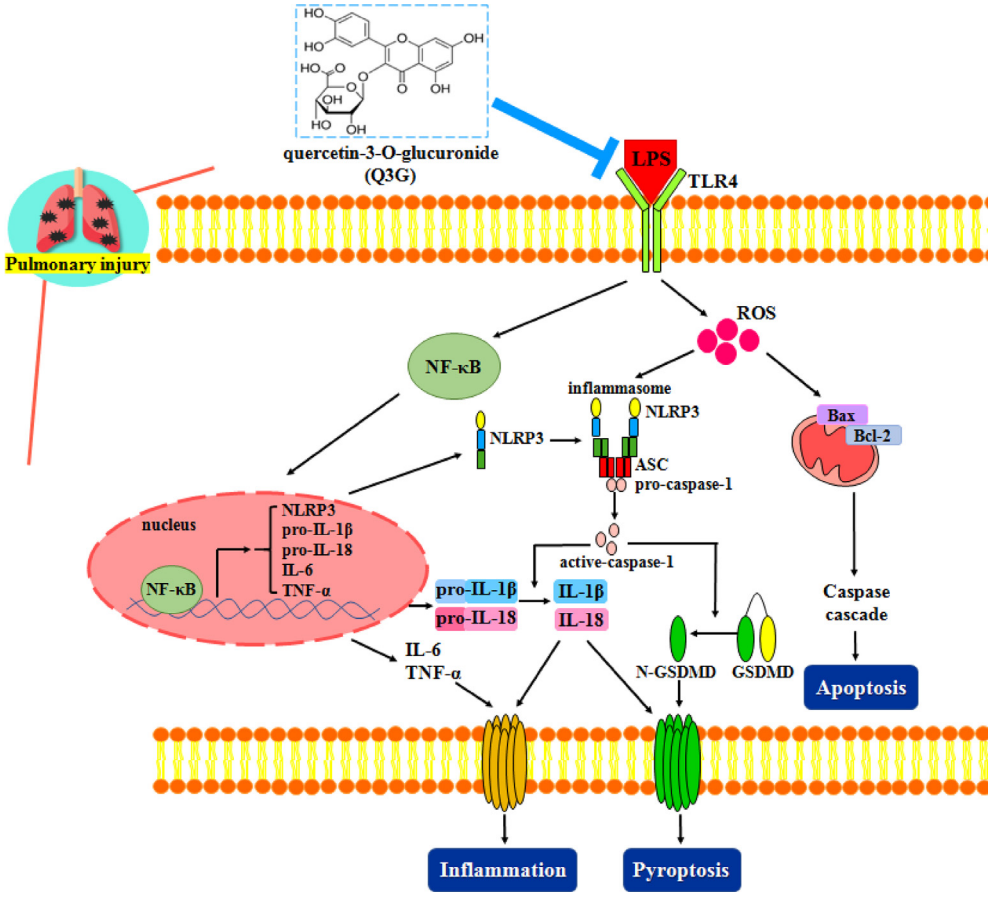

*Fig. 10. **Schematic representation of LPS-antagonist potential of Q3G on pulmonary injury.** LPS induces lung inflammation, pyroptosis and apoptosis through TLR4-mediated NF-κB signaling pathway and ROS production, then leading to activation of NLRP3 inflammasome and caspase cascade. Q3G functions against LPS via the inhibition of TLR4/NF-κB signaling, inactivation of NLRP3 inflammasome and downregulation of mitochondrial apoptosis pathway that subsequently alleviates the pulmonary injury.*

LPS has been commonly used and recommended as a tool to mimic the pulmonary injury in cultured cells and animals [6,50]. In this study, MRC-5 cells were treated with LPS (10 μg/mL) and C57BL/6 mice were injected by LPS/E as previously described [29] to establish *in vitro* and *in vivo* models of pulmonary injury. It has been demonstrated that LPS actives inflammatory responses through TLR4/NF-κB signaling, accompany with the elevation of oxidative stress [51]. Moreover, LPS accelerates the release of pro-inflammatory cytokines and the over-production of ROS in the lung cells during bacterial infections [7]. Extensive oxidative stress and ROS formation may active the NLRP3 inflammasome, leading to pyroptosis [52]. Apoptosis and mitochondrial dysfunction are also involved in the LPS-induced pulmonary injury [11]. In our study, LPS has been confirmed to induce cell survival loss, ROS generation (Figs. 1–2), an increase in release of pro-inflammatory cytokines such as IL-1β, IL-6 and TNFα, activation of TLR4/NF-κB signaling, NLRP3 inflammasome and pyroptosis (Fig. 3), as well as apoptosis (Figs. 4–5), as these prior observations. Instead, pre-treatment with Q3G at 0.25 μM could significantly reverse the increases in the above-mentioned cell abnormalities induced by LPS. The results from our study indicated that Q3G at lower concentrations (0.25 μM) had a protective effect via inhibition of inflammation and apoptosis in human lung fibroblasts MRC-5 cells (Figs. 2–5), and, on the other hand, a higher dosage (10–100 μM) suppressed MAPK pathway-mediated inflammatory responses in murine macrophages RAW 264.7 [25]. The findings, hence, provided evidences supporting bifunctions of Q3G on fibroblasts and macrophages between low and high doses, suggesting that Q3G may be more sensitive and effective in fibroblasts. It is worthy to study the effect of Q3G on fibroblasts combined with macrophages in a co-culture after LPS challenge, with regards to fibroblast-to-myofibroblast transition (FMT) and pulmonary fibrosis [53]. The hypothesis is that a co-culture model of the

human lungs composed of fibroblasts and macrophages would permit to a more precise evaluation of the Q3G's protective effects than the respective culture.

To further examine the underlying mechanisms of Q3G protection on MRC-5 cells from LPS damage, the crucial inflammatory, pyroptotic and apoptotic factors were evaluated, as shown in Figs. 3–5. NLRP3 inflammasome that provides a link between inflammation, pyroptosis and apoptosis, which may explain the multiple and abundant regulations operated by Q3G *in vitro*. Nosaka et al. (2020) has demonstrated that in a model of acute lung injury, autophagy down-regulates the NLRP3 activation to have an inhibitory effects on increased oxidative stress and secretion of IL-1β [54]. Past studies have revealed that autophagy plays a vital role during pulmonary injury because it not only represents deleterious effects under certain disease states, but also serves as a cellular protective mechanism [55,56]. To date, autophagy has been explored the regulation and functional significance in human lung diseases [57], and most studies focus on crucial autophagic mediators and their protective effects cross talk with the pathophysiology of pulmonary injury which may be regarded as therapeutic targets in lung diseases [58]. Future experiments will test the possible correlation between Q3G and autophagy to interfere the activation of NLRP3 inflammasome on this LPS model.

It is well-established an *in vivo* model for induction of pulmonary injury, more similar to COPD, was performed by employing a LPS/E-induced protocol [29]. Although LPS is the predominant risk factor of COPD, it is considered as one of the most commonly used rodent inducer for ARSD [6]. LPS has been applied in acute lung injury and demonstrated to result in inflammation, as well as especially in co-administered with elastase, chronic emphysema lesion display in lung tissues of mice [59]. It has been indicated that mice exposed to LPS/E construct structural and functional features typical of human COPD [60]. In agreement with the reports, this *vivo* experiments have revealed the LPS/E-treated mice developed a strong pulmonary injury and inflammation characterized by impairment in pulmonary function (Fig. 6), lung edema, emphysema and apoptosis (Figs. 7–8), as well as increased expressions of pro-inflammatory cytokines and activity of MPO (Fig. 9), which are features of exacerbations in chronic pulmonary injury in human [61]. Most significantly, *in vivo* intervention of Q3G improved the above-mentioned characteristics of pulmonary injury in the LPS/E-treated mice (Fig. 10). In comparison with Q3G and Dex, Q3G and Dex markedly lowered the destructive index of alveolar (Fig. 8C), and TUNEL-positive cells in lungs (Fig. 8D), suggesting the Q3G exhibited the *in vivo* inhibitory effects on cell injury and apoptosis comparable to that of Dex (Table S3). However, Dex is less responsive for reduction of IL-1β and TNFα, and MPO activity in this *in vivo* model (Fig. 9A and B). Moreover, In accordance with the safe dose of Dex [26], MRC-5 cells were treated with Q3G (0.125 or 0.25 μM), or Dex (10 μM), and then co-incubated with LPS (10 μg/mL) for 24 h to explore the effects of Q3G verse Dex *in vitro* by the morphologic observation, cell viability assay, and ROS analysis, as well as Annexin V/7-AAD double staining. In the LPS-stimulated MRC-5 cells, it was found the inhibitory effects of Q3G on cell survival loss, ROS production, and apoptosis were better than Dex (Fig. S2). Our data imply that Q3G might possess inhibitory potential on pulmonary injury better than a steroid medicine, and be used as a chemopreventive agent of pulmonary injury.

Additionally, the toxicity of Q3G was examined *in vivo*. Besides serum biochemical parameters of liver and renal functions and the ratio of organ weight to bw. (Tables 1 and 2), there was no significant difference in the alterations of pulmonary functions and physiologic status (Fig. 6), as well as IL-1β, IL-6 and TNF-α levels in the lung tissue (Fig. 9A) of the Q3G alone group when compared to the control group. Taken together, the normal weight and blood indexes of Q3G-treated mice suggested that the compound intervention had no obvious side effects *in vivo*. However, further studies exploring a full complement of toxic evaluation for the compound in animals ought to be encouraged for clinical translation in future. In conclusion, the findings provided that Q3G could attenuate inflammation, pyroptosis and apoptosis in pulmonary injury and COPD.

Conflicts of interest statement

The authors declare no conflict of interest.

Acknowledgments

This study was supported by the grant from the National Science and Technology Council (NSTC111-2320-B-040-020), Taiwan.

Appendix A

Table S1. The information of ISO 10993-5:2009 test for in vitro cytotoxicity of Q3G.

Content	Parameter
Test sample	**Quercetin-3-glucuronide (Q3G**, CAS no. 22688-79-5; purity >98.0%) was purchased from ChemFaces (Wuhan, Hubei, China), and prepared the stock concentration (100 mM) that was dissolved in sterilized water.
Cell line	**Human lung fibroblast cells MRC-5** were purchased from the Bioresource Collection and Research Center (BCRC, Food Industry Research and Development Institute, Hsinchu, Taiwan).
Medium	**Minimal Essential Medium with Earle's (MEM)** supplemented with 2.2 g/L sodium bicarbonate ($NaHCO_3$), 10% fetal bovine serum (FBS), 1% L-glutamine, 1% sodium pyruvate, 1% non-essential amino acids and 1% penicillin-streptomycin
Condition	The cell culture was maintained at a humidified incubator at 37 °C with 5% CO_2. Before treatments, **MRC-5 cells were starved in MEM without FBS for 24 h. Afterwards, the cells were incubated with various doses of Q3G (from 0.0025 to 25 μM) for 24 h.**
Test	**Information**
Method	**Direct contact test**
Assay	**1. Microscopic observation of cell morphology** **2. Cell viability by Muse™ Cell Analyzer** **3. Cell death assay (Annexin V/7-AAD assay)**
Control	**Negative control: untreated group**
Cellular response	**1. Nocytotoxic response in the groups of Q3G at dose ranges between 0.0025–0.25 μM** **2. Mildly cytotoxic response in the groups of Q3G at doses > 0.25 μM**

Table S2. Qualitative morphological grading of cytotoxicity based on the rules of ISO 10993-5:2009.

Grade	Reactivity	Conditions of all cultures
0	None	Discrete intracytoplasmatic granules, no cell lysis, no reduction of cell growth.
1	Slight	Not more than 20% of the cells are round, loosely attached and without intracytoplasmatic granules, or show changes in morphology; occasional lysed cells are present; only slight growth inhibition observable.
2	Mild	Not more than 50% of the cells are round, devoid of intracytoplasmatic granules, no extensive cell lysis; not more than 50% growth inhibition observable.
3	Moderate	Not more than 70% of the cell layers contain rounded cells or are lysed; cell layers not completely destroyed, but more than 50% growth inhibition observable.
4	Severe	Nearly complete or complete destruction of the cell layers.

Table S3. Comparison of the effects of Q3G verse Dex on cell survival, oxidative stress, and apoptosis under LPS challenge in vitro and in vivo.

Treatment[a]	Effect					
	Cell survival		Oxidative stress		Apoptosis	
	in vitro	*in vivo*	*in vitro*	*in vivo*	*in vitro*	*in vivo*
	Cell viability assay	Destructive index	ROS analysis	TBARS	Annexin V/7-AAD analysis	TUNEL stain
Q3G	140.77%** (↑)[b]	58.52%** (↓)	100.25%** (↓)	124.09%** (↓)	65.00%** (↓)	63.60%** (↓)
Dex	9.60% (↑)	56.97%** (↓)	63.79% (↓)	115.10%** (↓)	55.48%* (↓)	48.12%* (↓)

[a] The Q3G or Dex treatments were described in Materials and Methods.

[b] Each value is expressed as the mean (n = 3) of inhibition (↓) rate or induction (↑) rate, which were calculated in Q3G (0.25 μM) or Dex (10 μM) group compared with the LPS group *in vitro*, and in Q3G (0.15 μmol/mouse) or Dex (1 mg/kg) group compared with the LPS in combination with elastase (LPS/E) group *in vivo*, respectively. *$p < 0.05$, **$p < 0.01$ compared with the LPS or LPS/E group.

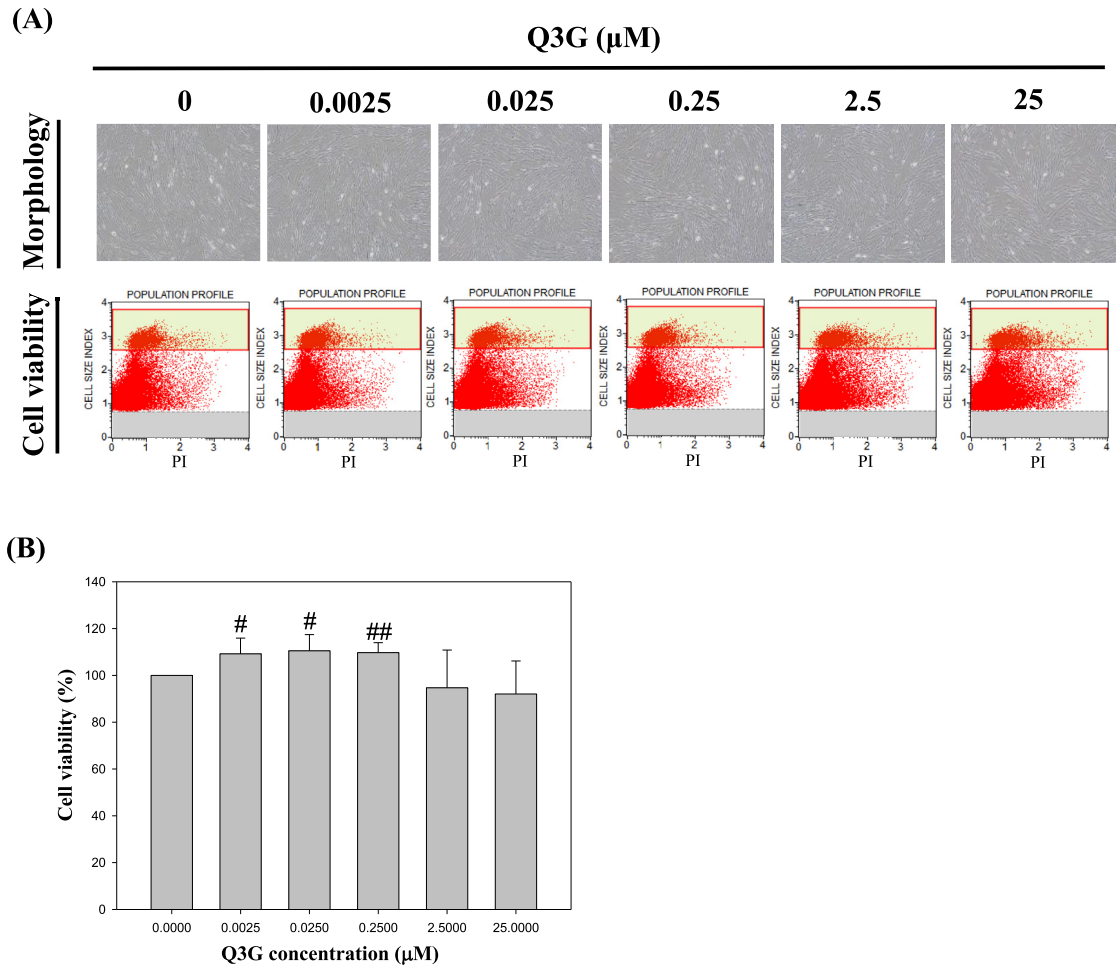

Fig. S1. ***Dose-screening effect of Q3G on cell morphology and viability in MRC-5 cells.*** ***(A)*** *Representative photomicrographs of MRC-5 cells were treated with various concentrations of Q3G (0, 0.0025, 0.025, 0.25, 2.5 and 25 μM) for 24 h (100x, upper panel). The cell viability was measured by Muse™ Cell Analyzer with PI stain (lower panel).* ***(B)*** *The quantitative data were presented as mean ± SD (n = 3) from three independent experiments.* $^{\#}p < 0.05$, $^{\#\#}p < 0.01$ *compared with the control group via one-way ANOVA with post-hoc Dunnett's test.*

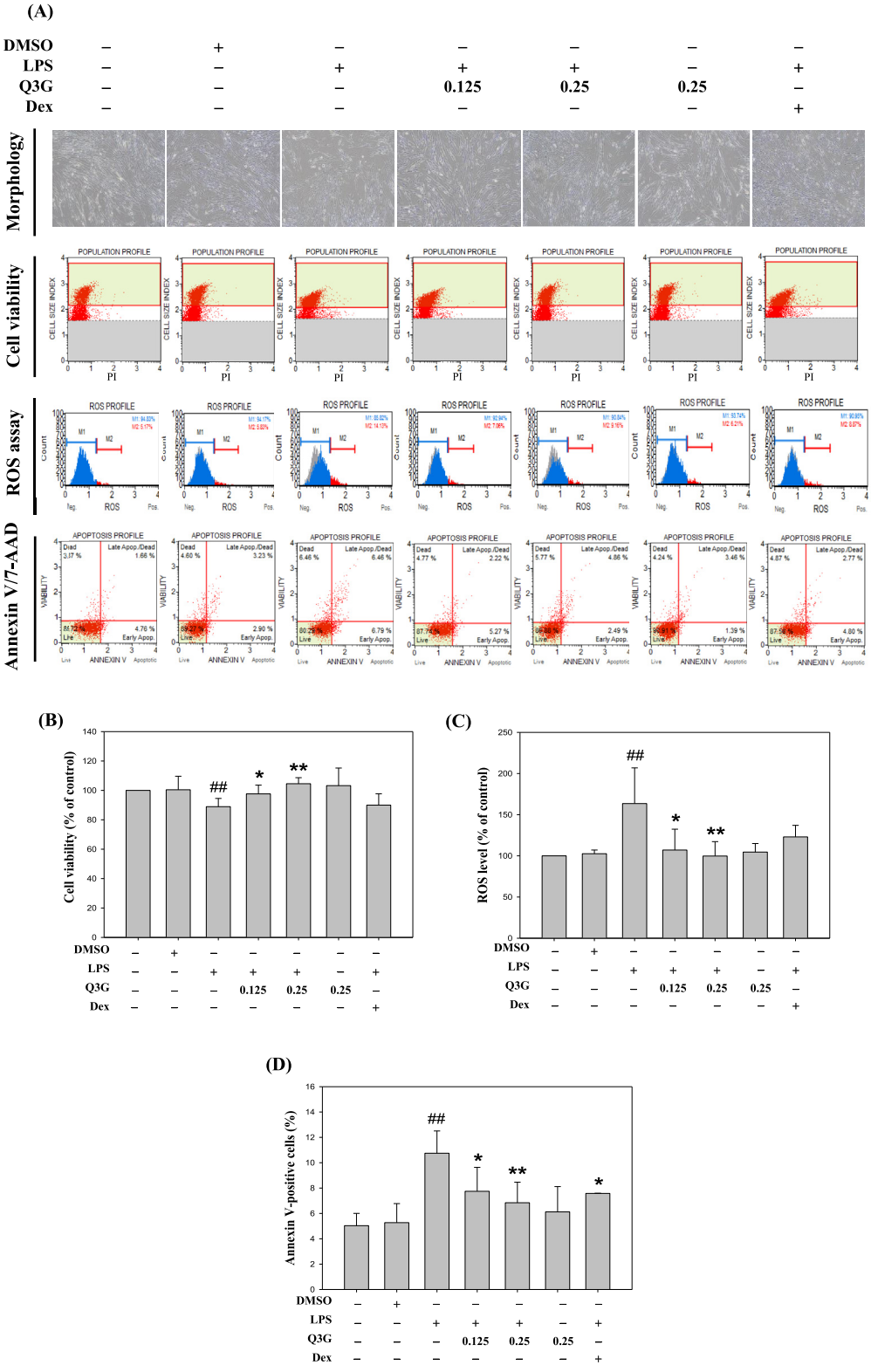

Fig. S2. ***Effects of Q3G and Dex on the LPS-induced cell survival loss, ROS generation and apoptosis in MRC-5 cells.*** ***(A)*** *Representative photomicrographs of MRC-5 cells were pre-treated with or without Q3G (0.125 μM or 0.25 μM) or Dex (10 μM) for 6 h, and then co-incubated with LPS (10 μg/mL) for another 24 h (100x, panel 1). The cell viability (panel 2), the ROS level (panel 3) and the annexin V/7-AAD staining (panel 4) were measured by Muse™ Cell Analyzer with PI stain, Oxidative stress, and Muse Annexin V & Dead Cell kits. The quantitative data of cell viability* ***(B)****, ROS content* ***(C)*** *and Muse™ Cell Analyzer assay of plasma membranes with annexin V/7-AAD staining, a significant number of total apoptotic cells were stained with positive annexin V-FITC and 7-AAD (right quadrant)* ***(D)*** *were presented as mean ± SD (n = 3) from three independent experiments. ##p < 0.01 compared with the control group via student's t-test. *p < 0.05, **p < 0.01 compared with the LPS group via student's t-test.*

References

[1] Berry CE, Wise RA. Mortality in COPD: causes, risk factors, and prevention. COPD 2010;7:375–82.
[2] Halpin DM, Miravitlles M, Metzdorf N, Celli B. Impact and prevention of severe exacerbations of COPD: a review of the evidence. Int J Chron Obstruct Pulmon Dis 2017;12: 2891–908.
[3] Johnson ER, Matthay MA. Acute lung injury: epidemiology, pathogenesis, and treatment. J Aerosol Med Pulm Drug Deliv 2010;23:243–52.
[4] Larsson L, Szponar B, Pehrson C. Tobacco smoking increases dramatically air concentrations of endotoxin. Indoor Air 2004;14:421–4.
[5] Wang HM, Bodenstein M, Markstaller K. Overview of the pathology of three widely used animal models of acute lung injury. Eur Surg Res 2008;40:305–16.
[6] Domscheit H, Hegeman MA, Carvalho N, Spieth PM. Molecular dynamics of lipopolysaccharide-induced lung injury in rodents. Front Physiol 2020;11:36.
[7] Chow C-W, Herrera Abreu MT, Suzuki T, Downey GP. Oxidative stress and acute lung injury. Am J Respir Cell Mol Biol 2003;29:427–31.
[8] Gross O, Thomas CJ, Guarda G, Tschopp J. The inflammasome: an integrated view. Immunol Rev 2011;243:136–51.
[9] Grailer JJ, Canning BA, Kalbitz M, Haggadone MD, Dhond RM, Andjelkovic AV, et al. Critical role for the NLRP3 inflammasome during acute lung injury. J Immunol 2014;192: 5974–83.
[10] Bannerman DD, Goldblum SE. Mechanisms of bacterial lipopolysaccharide-induced endothelial apoptosis. Am J Physiol Lung Cell Mol Physiol 2003;284:L899–914.
[11] Martin TR, Hagimoto N, Nakamura M, Matute-Bello G. Apoptosis and epithelial injury in the lungs. Proc Am Thorac Soc 2005;2:214–20.
[12] Ishizawa K, Yoshizumi M, Kawai Y, Terao J, Kihira Y, Ikeda Y, et al. Pharmacology in health food: metabolism of quercetin in vivo and its protective effect against arteriosclerosis. J Pharmacol Sci 2011;115:466–70.
[13] Manach C, Morand C, Crespy V, Demigné C, Texier O, Régérat F, et al. Quercetin is recovered in human plasma as conjugated derivatives which retain antioxidant properties. FEBS Lett 1998;426:331–6.
[14] Li Y, Yao J, Han C, Yang J, Chaudhry MT, Wang S, et al. Quercetin, Inflammation and Immunity. Nutrients 2016;8:167.
[15] Costa LG, Garrick JM, Roquè PJ, Pellacani C. Mechanisms of neuroprotection by quercetin: counteracting oxidative stress and more. Oxid Med Cell Longev 2016;2016:2986796.
[16] Wang W, Sun C, Mao L, Ma P, Liu F, Yang J, et al. The biological activities, chemical stability, metabolism and delivery systems of quercetin: a review. Trends Food Sci Technol 2016;56:21–38.
[17] Berkel Kaşõkçõ M, Bağdatlõoğlu N. Bioavailability of quercetin. Curr Res Nutr Food Sci J 2016;4:146–51.
[18] Yang HH, Hwangbo K, Zheng MS, Cho JH, Son JK, Kim HY, et al. Quercetin-3-O-β-D-glucuronide isolated from Polygonum aviculare inhibits cellular senescence in human primary cells. Arch Pharm Res 2014;37:1219–33.
[19] Terao J, Yamaguchi S, Shirai M, Miyoshi M, Moon J-H, Oshima S, et al. Protection by quercetin and quercetin 3-O-β-D-glucuronide of peroxynitrite-induced antioxidant consumption in human plasma low-density lipoprotein. Free Radic Res 2001;35:925–31.
[20] Shirai M, Moon JH, Tsushida T, Terao J. Inhibitory effect of a quercetin metabolite, quercetin 3-O-beta-D-glucuronide, on lipid peroxidation in liposomal membranes. J Agric Food Chem 2001;49:5602–8.
[21] Galindo P, Rodriguez-Gómez I, González-Manzano S, Dueñas M, Jiménez R, Menéndez C, et al. Glucuronidated quercetin lowers blood pressure in spontaneously hypertensive rats via deconjugation. PLoS One 2012;7:e32673.
[22] Wu Q, Needs PW, Lu Y, Kroon PA, Ren D, Yang X. Different antitumor effects of quercetin, quercetin-3'-sulfate and quercetin-3-glucuronide in human breast cancer MCF-7 cells. Food Funct 2018;9:1736–46.
[23] Guo X-D, Zhang D-Y, Gao X-J, Parry J, Liu K, Liu B-L, et al. Quercetin and quercetin-3-O-glucuronide are equally effective in ameliorating endothelial insulin resistance through inhibition of reactive oxygen species-associated inflammation. Mol Nutr Food Res 2013;57:1037–45.
[24] He YQ, Zhou CC, Yu LY, Wang L, Deng JL, Tao YL, et al. Natural product derived phytochemicals in managing acute lung injury by multiple mechanisms. Pharmacol Res 2021; 163:105224.
[25] Park JY, Lim MS, Kim SI, Lee HJ, Kim SS, Kwon YS, et al. Quercetin-3-O-β-D-glucuronide suppresses lipopolysaccharide-induced JNK and ERK phosphorylation in LPS-challenged RAW264.7 cells. Biomol Ther (Seoul) 2016;24: 610–5.
[26] Yap JMG, Ueda T, Kanemitsu Y, Takeda N, Fukumitsu K, Fukuda S, et al. AITC inhibits fibroblast-myofibroblast transition via TRPA1-independent MAPK and NRF2/HO-1 pathways and reverses corticosteroids insensitivity in human lung fibroblasts. Respir Res 2021;22:51.
[27] Standardization, I.O.f.. UNI EN ISO 10993-5:2009, "Biological Evaluation of medical devices—Part 5: in vitro cytotoxicity testing". Geneva, Switzerland: International Organization for Standardization; 2009.
[28] Yang Y, Song Z, Wu W, Xu A, Lv S, Ji S. ZnO quantum dots induced oxidative stress and apoptosis in HeLa and HEK-293T cell lines. Front Pharmacol 2020;11:131.
[29] Sichelstiel A, Yadava K, Trompette A, Salami O, Iwakura Y, Nicod LP, et al. Targeting IL-1β and IL-17A driven inflammation during influenza-induced exacerbations of chronic lung inflammation. PLoS One 2014;9:e98440.
[30] Liao Y-R, Lin J-Y. Quercetin intraperitoneal administration ameliorates lipopolysaccharide-induced systemic inflammation in mice. Life Sci 2015;137:89–97.
[31] Ni Y-L, Shen H-T, Su C-H, Chen W-Y, Huang-Liu R, Chen C-J, et al. Nerolidol suppresses the inflammatory response during lipopolysaccharide-induced acute lung injury via the modulation of antioxidant enzymes and the AMPK/Nrf-2/HO-1 pathway. Oxid Med Cell Longev 2019; 2019:9605980.
[32] Janbazacyabar H, van Bergenhenegouwen J, Verheijden KAT, Leusink-Muis T, van Helvoort A, Garssen J, et al. Non-digestible oligosaccharides partially prevent the development of LPS-induced lung emphysema in mice. Pharma Nutr 2019; 10:100163.
[33] Wang Q, Xiao L. Isochlorogenic acid A attenuates acute lung injury induced by LPS via Nf-κB/NLRP3 signaling pathway. Am J Transl Res 2019;11:7018–26.
[34] Thurlbeck WM. Measurement of pulmonary emphysema. Am Rev Respir Dis 1967;95:752–64.
[35] Saetta M, Shiner RJ, Angus GE, Kim WD, Wang NS, King M, et al. Destructive index: a measurement of lung parenchymal destruction in smokers. Am Rev Respir Dis 1985;131:764–9.
[36] Xie W, Wang H, Wang L, Yao C, Yuan R, Wu Q. Resolvin D1 reduces deterioration of tight junction proteins by upregulating HO-1 in LPS-induced mice. Lab Invest 2013;93: 991–1000.
[37] Liang Y, Miao Y, Xiang J. Circular RNA circESPL1 knockdown alleviates lipopolysaccharide (LPS)-induced lung cell injury via sponging miR-326 to regulate MAPK14. Int Immunopharm 2022;112:109146.
[38] Bock FJ, Tait SWG. Mitochondria as multifaceted regulators of cell death. Nat Rev Mol Cell Biol 2020;21:85–100.
[39] Sivandzade F, Bhalerao A, Cucullo L. Analysis of the mitochondrial membrane potential using the cationic JC-1 dye as a sensitive fluorescent probe. Bio-protocol 2019;9:e3128.
[40] Aratani Y. Myeloperoxidase: its role for host defense, inflammation, and neutrophil function. Arch Biochem Biophys 2018;640:47–52.

[41] Wu X, Kong Q, Zhan L, Qiu Z, Huang Q, Song X. TIPE2 ameliorates lipopolysaccharide-induced apoptosis and inflammation in acute lung injury. Inflamm Res 2019;68:981−92.
[42] Lee SY, Cho JH, Cho SS, Bae CS, Kim GY, Park DH. Establishment of a chronic obstructive pulmonary disease mouse model based on the elapsed time after LPS intranasal instillation. Lab Anim Res 2018;34:1−10.
[43] Rittirsch D, Flierl MA, Day DE, Nadeau BA, McGuire SR, Hoesel LM, et al. Acute lung injury induced by lipopolysaccharide is independent of complement activation. J Immunol 2008;180:7664−72.
[44] Li D, Ren W, Jiang Z, Zhu L. Regulation of the NLRP3 inflammasome and macrophage pyroptosis by the p38 MAPK signaling pathway in a mouse model of acute lung injury. Mol Med Rep 2018;18:4399−409.
[45] Thompson BT. Glucocorticoids and acute lung injury. Crit Care Med 2003;31:S253−7.
[46] Riley CM, Sciurba FC. Diagnosis and outpatient management of chronic obstructive pulmonary disease: a review. JAMA 2019;321:786−97.
[47] Lourenço SC, Moldão-Martins M, Alves VD. Antioxidants of natural plant origins: from sources to food Industry applications. Molecules 2019;24.
[48] Wei E, Fang X, Jia P, Li M, Jin P, Li F, et al. Ginsenoside Rb1 alleviates lipopolysaccharide-induced inflammatory injury by downregulating miR-222 in WI-38 cells. Cell Transplant 2021;30: 9636897211002787.
[49] Cong S, Xiang L, Yuan X, Bai D, Zhang X. Notoginsenoside R1 up-regulates microRNA-132 to protect human lung fibroblast MRC-5 cells from lipopolysaccharide-caused injury. Int Immunopharmacol 2019;68:137−44.
[50] Bals R. Lipopolysaccharide and the lung: a story of love and hate. Eur Respir J 2005;25:776.
[51] Nova Z, Skovierova H, Calkovska A. Alveolar-capillary membrane-related pulmonary cells as a target in endotoxin-induced acute lung injury. Int J Mol Sci 2019;20.
[52] Wang K, Zhang Y, Cao Y, Shi Z, Lin Y, Chen Y, et al. Glycyrrhetinic acid alleviates acute lung injury by PI3K/AKT suppressing macrophagic Nlrp3 inflammasome activation. Biochem Biophys Res Commun 2020;532:555−62.
[53] Sibinska Z, Tian X, Korfei M, Kojonazarov B, Kolb JS, Klepetko W, et al. Amplified canonical transforming growth factor-β signalling via heat shock protein 90 in pulmonary fibrosis. Eur Respir J 2017;49.
[54] Nosaka N, Martinon D, Moreira D, Crother TR, Arditi M, Shimada K. Autophagy protects against developing increased lung permeability and hypoxemia by down regulating inflammasome activity and IL-1β in LPS plus mechanical ventilation-induced acute lung injury. Front Immunol 2020;11:207.
[55] Mizumura K, Cloonan SM, Haspel JA, Choi AMK. The emerging importance of autophagy in pulmonary diseases. Chest 2012;142:1289−99.
[56] Mizumura K, Cloonan S, Choi ME, Hashimoto S, Nakahira K, Ryter SW, et al. Autophagy: friend or Foe in lung disease? Ann Am Thorac Soc 2016;13(Suppl 1):S40−7.
[57] Ryter SW, Choi AMK. Autophagy in the lung. Proc Am Thorac Soc 2010;7:13−21.
[58] Vishnupriya S, Priya Dharshini LC, Sakthivel KM, Rasmi RR. Autophagy markers as mediators of lung injury-implication for therapeutic intervention. Life Sci 2020;260:118308.
[59] Sajjan U, Ganesan S, Comstock AT, Shim J, Wang Q, Nagarkar DR, et al. Elastase- and LPS-exposed mice display altered responses to rhinovirus infection. Am J Physiol Lung Cell Mol Physiol 2009;297:L931−44.
[60] Ganesan S, Faris AN, Comstock AT, Chattoraj SS, Chattoraj A, Burgess JR, et al. Quercetin prevents progression of disease in elastase/LPS-exposed mice by negatively regulating MMP expression. Respir Res 2010;11:131.
[61] Drost EM, Skwarski KM, Sauleda J, Soler N, Roca J, Agusti A, et al. Oxidative stress and airway inflammation in severe exacerbations of COPD. Thorax 2005;60:293−300.